

# The Origin of Mass and the Nature of Gravity

Nassim Haramein<sup>†</sup>, Cyprien Guermonprez<sup>†</sup>, Olivier Alirol<sup>†</sup>

## Abstract

From the early explorations of thermodynamics and characterization of black body radiation, Max Planck predicted the existence of a non-zero expectation value for the electromagnetic quantum vacuum energy density or zero-point energy (ZPE). From the mechanics of a quantum oscillator, Planck derived the black body spectrum, which satisfied the Stefan-Boltzmann law with a non-vanishing term remaining where the summation of all modes of oscillations diverged to infinity in each point of the field. In modern derivation, correlation functions are utilized to derive the coherent behavior of the creation and annihilation operators. Although a common approach is to normalize the Hamiltonian so that all ground state modes cancel out, setting artificially ZPE to zero, zero-point energy is essential for the mathematical consistency of quantum mechanics as it maintains the non-commutativity of the creation and annihilation operators resulting in the Heisenberg uncertainty principle. From our computation, we demonstrate that coherent modes of the correlation functions at the characteristic time of the proton correctly result in the emergence of its mass directly from quantum vacuum fluctuation modes. We find as well that this energy value is consistent with a Casimir cavity of the same characteristic distance. As a result, we developed an analytical solution describing both the structure of quantum spacetime as vacuum fluctuations and extrapolate this structure to the surface dynamics of the proton to define a screening mechanism of the electromagnetic fluctuations at a given scale. From an initial screening at the reduced Compton wavelength of the proton, we find a direct relation to Einstein field equations and the Schwarzschild solution describing a source term for the internal energy of the proton emerging from zero-point electromagnetic fluctuations. A second screening of the vacuum fluctuations is found at the proton charge radius, which accurately results in the rest mass. Considering the initial screening, we compute the Hawking radiation value of the core Schwarzschild structure and find it to be equivalent to the rest mass energy diffusing in the internal structure of the proton. The resulting pressure gradient or pressure forces are calculated and found to be a very good fit to all the measured values of the color force and residual strong force typically associated to quark-antiquark and gluon flux tubes confinement. As a result, we are able to unify all confining forces with the gravitational force emerging from the curvature of spacetime induced by quantum electromagnetic vacuum fluctuations. Finally, we applied the quantum vacuum energy density screening mechanism to the observable universe and compute the correct critical energy density typically given for the total mass-energy of the universe.

## Introduction

General relativity demonstrates a relationship between mass-energy and the structure of spacetime that has real physical effects called gravity where massive objects, made of elementary particles producing their mass, curve spacetime resulting in a gravitational force. However, application of the same principles at the particles level yields gravitational forces that are so infinitely small that they are found to be insignificant. Yet, at the proton nuclear scale, extremely large confining forces are found which would require extremely high energy levels (or masses) to produce such a force in the context of general relativity. In fact, those very high levels of energy were actually predicted by early quantum field theory (QFT) resulting in the so-called 'bare mass' of particles but renormalized by modern quantum electrodynamics (QED) and quantum chromodynamics

---

<sup>†</sup> International Space Federation laboratory  
Email: research@spacefed.com

(QCD) utilizing quantum vacuum fluctuations as a shielding mechanism [1]. Consequently, one could ask the question in a different way than generally approached, that is, instead of why gravity is so weak, that has no meaning at the quantum level, but why is the proton mass, which is most of the mass of the material world, so small? This change in reasoning was eventually mentioned by others such as Franck Wilczek [2]. Furthermore, from deep studies of QFT and the divergence of the bare mass, one can ask a more fundamental question: is quantum vacuum fluctuations responsible for the bare mass shielding or is it the source of mass itself and resulting forces?

The general idea that mass is some kind of immutable value independent of forces and energies was dispelled in the early 1900 by the event of special and general relativity, when it was found that there is a fundamental equivalence between the concept of mass, energy and the geometry of space. General relativity establishes fundamental gravitational forces, which agglomerate particles and organized matter such as galaxies, stars, solar systems and planets, as the result of the curvature of the structure of space itself. However, this curvature results from an undefined source of energy, called mass, emerging from quantum entities we called particles. On the other hand, we have developed theories that describe these particles and energy structures as quantities emerging from very high energetic fields resulting from a fundamental oscillation of space itself we call quantum vacuum fluctuations, or ground state. These fields of 'virtual' particles are at the source of many of our modern particle theories of QFT, one of them being the Higgs field with a non-zero vacuum expectation value producing mass which only predicts  $\sim 1 - 5\%$  of the mass of the proton [3, 4], or for the explanation of orbital perturbation of an electron as in the Lamb shift. Consequently, both cosmological gravitational theory and quantum theory imbues very physical values to the structure of space itself with effects which have very fundamental and measurable attributes and which is intrinsically related to the concept of mass-energy.

Vacuum fluctuations or zero-point energy are predicted by the most precise theories in modern physics such as QFT, QED and QCD. However, the description of the electromagnetic vacuum fluctuations is still debated since the progressive and longstanding development from the early works from Planck and Einstein in early 1900 to recent publications providing further insights on the calculation of the vacuum fluctuations energy density as well as demonstrating its necessity for the mathematical consistency of quantum mechanics [1] and matter stability [5]. Confusion around vacuum fluctuations or zero-point energy (ZPE) arises from its many different uses throughout physics. Yet, their effects are measured experimentally (Casimir effect [6–8], Lamb shift [9], Vacuum Birefringence [10], etc.) and ZPE is considered as the source of creation and annihilation for real (spontaneous emission [11], electron-positron [12], Schwinger effect [13]) or virtual pairs (*dressed* particles, Feynman diagrams) of particles, and it corresponds to a ground state energy fields (Black body radiation [14]) or even a background field interacting with particles as in Lamb shift or electron self-energy (QED loop).

Here, we demonstrate that energy densities and thus masses are emerging properties of the fundamental dynamics of electromagnetic vacuum fluctuations. We reconcile these two views of the structure of space and demonstrate that mass-energy is an emergent property of spacetime at the quantum level that unifies gravity, the strong force at all scales under one mechanism<sup>1</sup>.

---

<sup>1</sup>**Note to the reader:** In this paper, we keep all units and do not utilize the common convention of reducing all the physical constant to one (where  $G = c = \hbar = 1$ ). While mathematically it could be convenient, it represents a loss of information and can lead to confusion [15]. Also, in certain cases, we do not reduce equations so that the physical meaning can be extracted clearly.

# 1 Zero-point energy and consequences

## 1.1 Origin and discovery of the ZPE

Zero-point energy (ZPE) was discovered from the study of the interaction between electromagnetic waves and condensed matter, examining the thermodynamics of black body radiation and the photoelectric effect. ZPE was first obtained by Max Planck trying to solve the UV-catastrophe present in the former classical models (Rayleigh-Jeans and Wien models) describing the energy density spectrum radiated by a black body observed by Kirchhoff in 1860 [16]. The objective was to understand, from a thermodynamics point of view, the mechanisms of absorption and radiation of electromagnetic frequency  $\nu$  of a black body held at a constant temperature  $T$ . These early attempts allowed in particular the derivation of the Stefan-Boltzmann law giving the radiative energy surface density  $j(T)$  (in  $\text{W.m}^{-2}$ ) as a function of the massive body temperature

$$j(T) = \sigma T^4 \quad (1.1)$$

where  $\sigma$  is the Stefan-Boltzmann constant.

From the classical model, Max Planck described atoms as harmonic oscillator cavities [14] and derived the radiated energy density  $B_\nu(T)d\nu$  (in  $\text{J.m}^{-3}$ ) in the frequency interval  $[\nu, \nu + d\nu]$ . By equating the absorption rate of an external electromagnetic energy by a black body and its emission rate he obtained the energy density spectrum

$$B_\nu(T) = \frac{8\pi\nu^2}{c^3}U, \quad (1.2)$$

where  $U$  is the total internal energy of the oscillator [16]. At the time, the challenge was the determination of the correct expression for  $U$ .

Although the oscillator is typically visualized as a linear oscillating spring, one must consider that the spring analogy is a 1D projection of a 3D rotational motion (Figure 1), the latter of which is a more realistic and precise visualization of what is occurring in the real physical resonators under consideration (e.g. atoms).

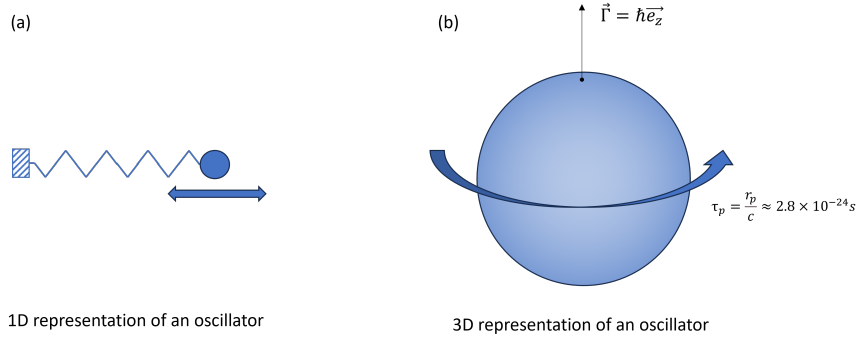


Figure 1: (a) Typical representation of an oscillator as a spring with a mass attached to it in a 1D oscillation. (b) More realistic representation of a natural oscillator as a 3D rotational motion.

Various statistically unsuccessful derivations such as the Rayleigh-Jeans or Wien distribution laws, were tried to compute an electromagnetic energy density spectrum compatible with the Stefan-Boltzmann law. The Rayleigh-Jeans solution  $\tilde{B}_\nu(T) = \frac{8\pi\nu^2}{c^3}k_B T$  produced the ultraviolet divergence while the Wien  $B_\nu(T) = \frac{8\pi\nu^3 h}{c^3} e^{-\frac{h\nu}{k_B T}}$  distribution had no divergence but failed to compute the correct value for the Stefan-Boltzmann constant. Following these early attempts, Planck initially started by applying the laws of thermodynamics to the black body and related the total energy  $U$  to the system entropy  $S$ . His major assumption was to consider

a continuous absorption and emission, with each individual oscillator emitting an elementary energy  $\epsilon$  proportional to its internal frequency  $\nu$ ,  $\epsilon = h\nu$  [5]<sup>2</sup>. Planck thus obtained a total internal energy

$$U = \frac{h\nu}{e^{\frac{h\nu}{kT}} - 1} \quad (1.3)$$

From which, in 1901, he deduced the solution matching the experimental data known as Planck's law.

$$B(\nu, T) = 8\pi \frac{h\nu^3}{c^3} \frac{1}{e^{\frac{h\nu}{kT}} - 1} \quad (1.4)$$

This first law resolved the UV-catastrophe with a finite spectrum at high frequencies and the corresponding radiative energy density giving the Stefan-Boltzmann law. However, it raised a new issue as the internal energy  $U$  should reduce to  $k_B T$  as predicted by the equipartition theorem in the classical limit of high temperatures  $k_B T \gg h\nu$

$$U = \frac{h\nu}{e^{\frac{h\nu}{kT}} - 1} \approx \frac{h\nu}{1 + \frac{h\nu}{k_B T} + \frac{1}{2} \left( \frac{h\nu}{k_B T} \right)^2 - 1} = \frac{k_B T}{1 + \frac{1}{2} \frac{h\nu}{k_B T}} \approx k_B T - \frac{1}{2} h\nu \quad (1.5)$$

From the Taylor series development, Planck found an additional negative term of  $-\frac{1}{2}h\nu$  corresponding to a missing contribution. Even though his law was successfully matching the experimental density spectrum, Planck was not satisfied by its derivation due to this negative residual term. It took him almost ten years to develop a new theory. In the meantime, by studying the emission of electrons from metals illuminated by light, now known as the photoelectric effect, Albert Einstein proposed, in 1905, that the quantum term discovered by Planck was a real physical attribute of radiation and elementary absorbers, such that a beam of light propagates in discrete energy packets comprised of energy quanta  $h\nu$ , which he coined photons. This finding of discrete emission of light as photons by matter led to Planck's second proposition.

In 1912, Planck's second theory described the black body as a system of elementary oscillators able to continuously absorb light but radiate a discrete (quantized) electromagnetic energy  $nh\nu$  [5]<sup>3</sup>. Planck proposed that an oscillator would absorb continuously until it reached a certain energy threshold from which it emitted a quanta with a defined probability. Thus, he derived a new expression for the internal energy  $U$

$$U = \frac{h\nu}{2} \frac{e^{\frac{h\nu}{kT}} + 1}{e^{\frac{h\nu}{kT}} - 1} = \frac{h\nu}{e^{\frac{h\nu}{kT}} - 1} + \frac{1}{2} h\nu, \quad (1.6)$$

Here appears a second terms  $\frac{1}{2}h\nu$  which corresponds to the missing contribution, in addition to the classical term  $\frac{h\nu}{e^{\frac{h\nu}{kT}} - 1}$  previously derived ten years earlier. Therefore, Planck's second theory satisfies the equipartition theorem resulting in  $U \approx k_B T$  at high temperature ( $k_B T \gg h\nu$ )

$$U = \frac{h\nu}{e^{\frac{h\nu}{kT}} - 1} + \frac{1}{2} h\nu \approx k_B T - \frac{1}{2} h\nu + \frac{1}{2} h\nu \approx k_B T \quad (1.7)$$

However, this new term meant as well, that even at zero Kelvin ( $T \rightarrow 0K$ ), oscillations still occurs resulting in what Planck coined zero point energy (ZPE) corresponding to a ground state energy  $U_0$

$$U_0 = \frac{1}{2} h\nu \quad (1.8)$$

---

<sup>2</sup>p.5-7  
<sup>3</sup>p.687

Due to the discrete emission mechanism, Planck thought he could no longer utilize Equation (1.2) to obtain the energy density spectrum as it was derived in the case of a continuous emission. Planck thus considered that the ratio between the probability of not emitting ( $1 - p$ ) and the probability to emit ( $p$ ) a light quanta is proportional to the energy density spectrum  $B_\nu(T)$  and obtained once again his 1901 law (Eq (1.4)). In his second theory, Planck obtained the right expression for the energy  $U$ , which includes ZPE. He believed ZPE would not have much experimental consequences [5]<sup>4</sup>, however as we will see ZPE is involved in the critical fundamental phenomena of quantum mechanics such as spontaneous emission, Lamb shift and many others (see Table 1 & [17]). At that time, the ZPE did not appear in Planck's law for the energy density spectrum  $B_\nu(T)$  (as  $B_\nu(T) \rightarrow 0$  when  $T \rightarrow 0$ ), although in modern course text books the ZPE density spectrum is considered for the free field (or vacuum). This idea of vacuum fluctuations (ZPE) also came a few years later, in 1916, by Walther Nernst who replaced the  $k_B T$  term in Rayleigh-Jeans distribution by  $\hbar\nu$  to estimate the zero-point energy spectrum of the free electromagnetic field. To avoid the UV-divergence of the energy density, Nernst had to introduce a cut-off frequency  $\nu_m$  such that

$$\rho(\nu_m) = \int_0^{\nu_m} \tilde{B}_0(\nu) d\nu = \frac{2\pi\hbar}{c^3} \nu_m^4 \quad (1.9)$$

Nernst realized that the vacuum ZPE was “quite enormous, making extraordinary fluctuations in it to exert great actions” [18].

To derive the complete expression of the energy density spectrum  $B_t(\nu, T)$  which includes the black body spectrum and the vacuum spectrum, Planck could have combined Equation (1.2) and (1.6) to obtain the total energy spectrum

$$B_t(\nu, T) = B(\nu, T) + B_0(\nu) = 8\pi \frac{\hbar\nu^3}{c^3} \frac{1}{e^{\frac{\hbar\nu}{kT}} - 1} + 4\pi \frac{\hbar\nu^3}{c^3} \quad (1.10)$$

in which the vacuum energy spectrum of the free electromagnetic field  $B_0(\nu) = 4\pi \frac{\hbar\nu^3}{c^3}$  appears as suggested by Nernst.

## 1.2 Modern derivation of ZPE in free electromagnetic field

The modern derivation of the  $B_\nu(T)$  uses quantum field theory [1]<sup>5</sup> and correlation functions between destructive and constructive interference (see Appendix A & B for details). The correlation function is a way to measure the coherence of the field [19]. The energy density of the electromagnetic field for a normally ordered correlation function is

$$\left\langle \vec{E}^{(-)}(\vec{r}, t) \cdot \vec{E}^{(+)}(\vec{r}, t + \tau) \right\rangle = \frac{\hbar}{2\pi^2\epsilon_0 c^3} \int_0^\infty \frac{d\omega \omega^3 e^{-i\omega\tau}}{e^{\hbar\omega/kT} - 1} \quad (1.11)$$

In a coherent system, positive (absorption/photon annihilation) and negative (emission/photon creation) frequencies are considered resulting in a symmetrically ordered correlation function

$$\begin{aligned} \left\langle \vec{E}(\vec{r}, t) \cdot \vec{E}(\vec{r}, t + \tau) \right\rangle &= \left\langle \vec{E}^{(-)}(\vec{r}, t) \cdot \vec{E}^{(+)}(\vec{r}, t + \tau) \right\rangle + \left\langle \vec{E}^{(+)}(\vec{r}, t) \cdot \vec{E}^{(-)}(\vec{r}, t + \tau) \right\rangle \\ &= \frac{\hbar}{\pi^2\epsilon_0 c^3} \int_0^\infty \frac{d\omega \omega^3 \cos \omega\tau}{e^{\hbar\omega/kT} - 1} + \frac{\hbar}{2\pi^2\epsilon_0 c^3} \int_0^\infty d\omega \omega^3 e^{i\omega\tau} \end{aligned} \quad (1.12)$$

When the field modes are sufficiently coherent (the characteristic time is very small,  $\tau \approx 0$ ), the electromagnetic

---

<sup>4</sup>p.11

<sup>5</sup>p.180-182

energy density  $\rho(T)$  (in  $\text{J.m}^{-3}$ ) derived from the expectation value of the electric free field is

$$\begin{aligned}\rho(T) &= \epsilon_0 \langle E^2(\vec{r}, t) \rangle \\ &= 8\pi \frac{\hbar}{c^3} \int_0^\infty \left( \frac{1}{e^{\frac{\hbar\nu}{kT}} - 1} + \frac{1}{2} \right) \nu^3 d\nu \\ &= \int_0^\infty (B(\nu, T) + B_0(\nu)) d\nu \\ &= \frac{4}{c} \sigma T^4 + \int_0^\infty B_0(\nu) d\nu\end{aligned}\tag{1.13}$$

with  $\sigma = \frac{\pi^2 k^4}{60 \hbar^3 c^2}$  the Stefan-Boltzmann constant. This complete expression of the energy density contains two terms : the first term corresponds to the Stefan-Boltzmann law, and the second term representing ZPE arises only at coherent scales. ZPE density is given by

$$\rho_{vac} = \int_0^\infty B_0(\nu) d\nu\tag{1.14}$$

which displays a divergence at high frequencies. This is resolved by regularizing the field with a cut-off frequency as shown in section 2.2.

These early derivations by Planck, Einstein and Nernst on the interaction between light and matter yielding the ZPE density are at the roots of quantum mechanics. The treatment of the harmonic oscillators intrinsically predicts the existence of a non-zero ground state energy of the vacuum which is apparent in the eigenvalues of the harmonic oscillators Hamiltonian (see section 1.3). Also, the vacuum electromagnetic energy  $\rho_{vac}$  is critical for the treatment of the bare mass and charge and the renormalization process utilized in quantum electrodynamic (QED) and quantum chromodynamics (QCD).

Historically, the work on the absorption and emission of an electromagnetic field by matter was extended by Dirac in 1927 in his quantum electrodynamics theory of the electron describing the interaction of charged particles by the means of photons being quantized excitations of the electromagnetic field, typically described as a quantum field theory (QFT). According to QFT, the zero-point energy appears in every single field as in QED vacuum and QCD vacuum and describes particles as excited states of their respective fields giving a description of particle creation and interaction. However, the Standard Model does not address the gravitational field and the spacetime structure associated with energy density levels resulting from a non-zero vacuum energy (i.e. ZPE). John Archibald Wheeler and others treated some of these issues, which will be discussed in sections 2.

In the following, we will highlight how ZPE is a necessity in both theoretical approaches and experimental results analysis for consistency.

### 1.3 ZPE in Quantum mechanics and its necessity for mathematical consistency

The elucidation of the electromagnetic field in the vacuum state can be deduced from quantum mechanics. An electromagnetic field in vacuum is typically treated mathematically as a one dimensional harmonic oscillator, a model broadly used in quantum mechanics especially in perturbation theory [5]<sup>6</sup>. The generic quantum Hamiltonian for a harmonic oscillator is

$$\hat{H} = \frac{\hat{p}^2}{2m} + \frac{1}{2} m\omega^2 \hat{x}^2\tag{1.15}$$

with  $m$  the particle mass,  $\hat{p} = -i\hbar\nabla$ . the momentum operator,  $\hat{x}$  the position operator and  $\omega = \sqrt{k/m}$  the typical oscillator of force  $k$  frequency. While working on the coefficient of spontaneous emission of an atom [11], Dirac derived from the non-commutative rule  $[\hat{x}, \hat{p}] = i\hbar$  a whole theory of operators mechanics which yields to the definition of the annihilation  $a$  and creation  $a^\dagger$  operators based on the position and

---

<sup>6</sup>p.36-41

momentum operators such that  $[a, a^\dagger] = 1$  and the harmonic oscillator Hamiltonian can be simplified as (see Appendix A)

$$\hat{H} = \hbar\omega \left( a_\omega^\dagger a_\omega + \frac{1}{2} \right) \quad (1.16)$$

The associated Schrödinger equation can be solved by looking for the eigenstates of the number operator  $a^\dagger a$  from which time-independent energy level for the harmonic oscillator are deduced

$$E_n = \hbar\omega \left( n + \frac{1}{2} \right) \quad (1.17)$$

with  $n \in \mathbb{N}$ , the number of photons present in the mode  $|n\rangle$ . The ZPE corresponds to the ground state mode  $|0\rangle$ , which has no photon but still has an energy  $E_0 = \frac{1}{2}\hbar\omega$ . Therefore, the quantum theory of radiation predicts a zero point energy for the electromagnetic field.

The nature of ZPE can be further understood when translated into the quantization of vacuum electromagnetic field. As shown in Appendix A, the harmonic oscillators analysis yields the following electric and magnetic fields

$$\vec{E}(t) = -\frac{\partial \vec{A}}{\partial t} = i\sqrt{2\pi\hbar\omega} \left( a_\omega(t)\vec{A}_0(\vec{r}) - a_\omega^\dagger(t)\vec{A}_0^*(\vec{r}) \right) \quad (1.18)$$

$$\vec{B}(t) = \nabla \times \vec{A} = \sqrt{\frac{2\pi\hbar c^2}{\omega}} \left( a_\omega(t)\nabla \times \vec{A}_0(\vec{r}) - a_\omega^\dagger(t)\nabla \times \vec{A}_0^*(\vec{r}) \right) \quad (1.19)$$

In the vacuum state, and for all the stationary state  $|n\rangle$  the expectation values for the electric and magnetic field becomes 0

$$\langle \vec{E}(\vec{r}, t) \rangle_\tau = \langle \vec{B}(\vec{r}, t) \rangle_\tau = 0 \quad (1.20)$$

As expected, the electric and magnetic fields oscillate with a zero mean value illustrating the fact that they are not observed at our usual time scale ( $\tau \gg \tau_0$ ) since the coherent time  $\tau_0$  is very small. Historically, this has been described as a field of 'virtual' particles. However, the energy density calculated as the expectation value of the square of the electric field is non-zero

$$\langle E^2(\vec{r}, t) \rangle = 4\pi\hbar\omega |\vec{A}_0(\vec{r})|^2 n + \langle E^2(\vec{r}) \rangle_0 \quad (1.21)$$

with ZPE density given by

$$\epsilon_0 \langle E^2(\vec{r}) \rangle_0 = \frac{\hbar\omega}{2\mathcal{V}} \quad (1.22)$$

With no photon  $n = 0$ , the electromagnetic energy density  $\epsilon_0 \langle E^2(\vec{r}) \rangle_0$  remains lower than the quantum of energy  $\hbar\omega$  threshold for spontaneous emission.

ZPE can be and is commonly mathematically removed from the Hamiltonian by normal ordering procedure  $\hat{H}' = \hat{H} - E_0(\omega)$ , but this does not mean that ZPE vanishes from the system. In fact, the non-zero value of the  $|0\rangle$  mode results from the non-commutative relationship between operators  $a$  and  $a^\dagger$  ( $[a, a^\dagger] = 1$ ) and is essential for the mathematical consistency of quantum theory [5]<sup>7</sup>. This can be demonstrated when we consider a dipole model of the atom where the dipole length is represented by the coordinates  $x(t)$ . The resulting harmonic oscillator equation which takes into account the radiation reaction field  $\omega_0^2 \tau \dot{x}$  (in the small-damping approximation  $\omega_0 \tau \ll 1$ ) and the zero-point energy source  $\frac{e}{m} E_0(t)$  is

$$\ddot{x} + \omega_0^2 \tau \dot{x} + \omega_0^2 x = \frac{e}{m} E_0(t) \quad (1.23)$$

---

<sup>7</sup>p.53

with  $\tau = \frac{2e^2}{3mc^3\epsilon_0}$  and  $\omega_0$  the natural frequency of the system. The solution without ZPE ( $E_0(t) = 0$ ) predicts a rapid collapse of the dipole length ( $t \gg (\omega_0^2\tau)^{-1}$ ), like in the case of the classical electron in which it would radiate all its energy and fall on the nucleus [5] (p81)

$$x(t) = -x_0 e^{-\frac{\omega_0^2\tau}{2}t} (\cos(\omega t) + \sin(\omega t)) \xrightarrow[t \gg (\omega_0^2\tau)^{-1}]{} 0 \quad (1.24)$$

In fact, the ZPE is a source term necessary to the stability of matter, counterbalancing the radiative damping of the dipole. When considering a non-zero ZPE in the equation in the form of  $E_0(t) = E_{0\omega} \cos(\omega t + \theta)$ , we get

$$x(t) = -\frac{e}{m} \operatorname{Re} \left( \frac{E_{0\omega} e^{-i\omega t + \theta}}{(\omega^2 - \omega_0^2) + i\tau\omega^3} \right) \quad (1.25)$$

Also, this solution with the ZPE maintains the non-commutative relationship necessary for the mathematical consistency of quantum theory. In the small-damping approximation  $\omega_0\tau \ll 1$ , we can calculate the mean over time value for the commutator [5]<sup>8</sup>

$$\begin{aligned} [\hat{x}, \hat{p}] &= \langle x | [\hat{x}, \hat{p}] | x \rangle \\ &= \sum_{\omega} \frac{ie^2 E_{0\omega}^2}{m} \frac{\omega}{(\omega^2 - \omega_0^2)^2 + \tau^2 \omega^6} \end{aligned} \quad (1.26)$$

For isotropic and unpolarized vacuum fluctuations, we have  $E_{0\omega}^2 = \frac{8\pi}{3\epsilon_0} \mathcal{B}_0(\omega) d\omega$  such that, in the continuum mode limit where  $\sum_k \rightarrow \frac{V}{8\pi^3} \int d^3k$ , the commutative relationship can be approximated by (see Appendix C)

$$[\hat{x}, \hat{p}] \simeq \frac{i\hbar e^2}{2\pi^2 \epsilon_0 m c^3} \frac{8\pi}{3} \int_0^\infty \frac{d\omega \omega^4}{(\omega^2 - \omega_0^2)^2 + \tau^2 \omega^6} \simeq \frac{2i\hbar e^2 \omega_0^3}{3\pi m c^3 \epsilon_0} \frac{\pi}{\tau \omega_0^3} = i\hbar \quad (1.27)$$

Consequently, ZPE is required to maintain the non-commutativity of the operators  $[\hat{x}, \hat{p}] = i\hbar$  which leads to the fact that the Heisenberg uncertainty principle emerges from the vacuum fluctuations of the ZPE. These vacuum fluctuations are expressed by the position  $\sigma_x$  and momentum  $\sigma_p$  standard deviations which are computed from the number operator eigenvectors  $|n\rangle$ , as

$$\sigma_x^2 = \langle n | x^2 | n \rangle = \frac{i^2 \hbar}{2m\omega} \langle n | (a - a^\dagger)^2 | n \rangle = \frac{\hbar}{m\omega} \left( n + \frac{1}{2} \right) \quad (1.28)$$

and

$$\sigma_p^2 = \langle n | p^2 | n \rangle = \frac{\hbar m \omega}{2} \langle n | (a + a^\dagger)^2 | n \rangle = \hbar m \omega \left( n + \frac{1}{2} \right) \quad (1.29)$$

from which the Heisenberg principle is deduced

$$\sigma_x \sigma_p = \hbar \left( n + \frac{1}{2} \right) \geq \frac{\hbar}{2} \quad (1.30)$$

It then follows that the foundations of quantum mechanics and the uncertainty principle are firmly rooted in the dynamics of ZPE vacuum fluctuations that defines the bath (or field) in which particles appear, evolve

---

<sup>8</sup>p.54

and interact. Thus, contrary to popular belief, the uncertainty principle is a consequence, not the source of ZPE [5].

Furthermore, the attempts to resolve the divergence problems induced in quantum mechanics by ZPE, all the while utilizing it to define the fundamental fields of particles and forces, have not been successfully resolved by the renormalization process. This, in turn, led to very strong statements by some of the fathers of quantum mechanics

Most physicists are very satisfied with the situation. They say: 'Quantum electrodynamics is a good theory and we do not have to worry about it any more.' I must say that I am very dissatisfied with the situation because this so-called 'good theory' does involve neglecting infinities which appear in its equations, ignoring them in an arbitrary way. This is just not sensible mathematics. Sensible mathematics involves disregarding a quantity when it is small – not neglecting it just because it is infinitely great and you do not want it! **Dirac, 1975** [20]<sup>9</sup>

The shell game that we play is technically called 'renormalization'. But no matter how clever the word, it is still what I would call a dippy process! Having to resort to such hocus-pocus has prevented us from proving that the theory of quantum electrodynamics is mathematically self-consistent. It's surprising that the theory still hasn't been proved self-consistent one way or the other by now; I suspect that renormalization is not mathematically legitimate. **Feynman, 1985** [21]<sup>10</sup>

Attempts to renormalize infinities in quantum theory have consequences to the structure of spacetime, explored by many, and meet within black holes, at singularity, where spacetime diverges to infinity as a result of general relativity. In the last few decades, explorations of these consequences have been explored extensively in astrophysical applications of quantum mechanics from the holographic principle of Juan Maldacena [22], Gerard t'Hooft [23] and Leonard Susskind [24], to Wheeler's quantum foam [25], the virtual micro-black holes of Stephen Hawking [26] and a correspondence between quantum entanglement and spacetime as in Einstein-Rosen bridges (ER = EPR). Typically, in all of these explorations the renormalization problem in quantum mechanics is not addressed as the emphasis is on resolving issues of infinities and conservation in relativistic physics. Yet, there may be great insights in applications of spacetime formalism at the quantum scale to give physical meaning to regularization and renormalization.

In the sections below, we explore the relationship of ZPE to the structure of spacetime, its physical relevance and role in experimental work.

## 1.4 Experimental validations of the ZPE

Dirac's motivation to develop QED theory was mainly due to the calculation of the spontaneous emission rate in the hydrogen atom model initiated by Bohr to explain hydrogen spectral lines. In Bohr's model, the electron can only exist in certain, discretely separated orbits, where each transition results in spontaneous emission or absorption of a photon. When a photon is absorbed, it is annihilated by jumping into the vacuum state, while an emitted photon is created by jumping out of the vacuum state. Similarly, the electron jumps by being absorbed and emitted from the vacuum at its new orbit. This is mathematically seen through the annihilation and creation operators which are lowering or raising by one quantum the energy level of the system :  $a|n\rangle = \sqrt{n}|n-1\rangle$  and  $a^\dagger|n\rangle = \sqrt{n+1}|n+1\rangle$ . From Dirac's equation, a relativistic version of the Schrödinger equation, both positive and negative energy states are accessible by the electrons in which  $E = -c\sqrt{p^2 + m^2c^2}$  is as true as  $E = c\sqrt{p^2 + m^2c^2}$ . This observation led Dirac to postulate the existence of the Dirac sea as a pool of disposable electrons with negative energy that can appear out of the vacuum. From this conception Dirac successfully predicted the existence of the anti-electron, or positron, as a hole in the Dirac sea. In 1932, the positron existence was experimentally confirmed by Carl Anderson [12].

This capacity of creation and annihilation of electron-positron pairs out of the electromagnetic vacuum predicted by the Dirac equation and demonstrating the physicality of the quantum vacuum fluctuations, has been recently experimentally observed:

---

<sup>9</sup>p.184

<sup>10</sup>p.128

- **Schwinger effect:** when applying to the vacuum an electromagnetic field above the Schwinger limit ( $E_S = \frac{m_e^2 c^3}{e\hbar} = 1.32 \times 10^{18} \text{ V.m}^{-1}$ ), electron-positron pairs experience sufficient separation to overcome cyclical annihilation and are observed, the limit was first derived in 1931 in one of QED's earliest theoretical successes by Fritz Sauter [27] and later codified by Julian Schwinger who calculated the rate of electron-positron pair production [28]. This was measured in 2022 in graphene superlattices [13, 29].
- **Vacuum birefringence :** postulated by Schwinger in 1936, the vacuum birefringence is now experimentally observed around Isolated Neutron Stars (or pulsar). Pulsars generate extremely intense magnetic fields which are above the Schwinger limit such that electrons and positrons are being created out of the vacuum around the neutron star. The anisotropy of the vacuum in this region makes it birefringent, which can be observed in the measured polarization degree of light from the pulsar [30].
- **Breit-Wheeler effect :** two photons are combined to form an electron-positron pair, which has been experimentally measured in 2021 at the Large Hadron Collider [10].

One of the first and major experimental validation of the ZPE is attributed to the Lamb shift. In 1947, Lamb and Rutherford measured a shift in the hydrogen energy level  $2_{p_{1/2}}$  that was not expected by Dirac's equation. It was later found that the so-called Lamb shift is the result of vacuum energy fluctuations interacting with the electron around the nucleus [9]. It was a key observation of the effect of the ZPE and proved the physical impact of vacuum fluctuations.

Another experimental confirmation of the ZPE is the Casimir effect. When studying the attractive Van der Waals force between two atoms in vacuum, Hendrik Casimir discovered that two mirrors in vacuum experience a force due to the cavity between the plates eliminating a percentage of the vacuum fluctuations modes producing an energy gradient resulting in a force [31]. Steven Lamoreaux in 1997 first measured the effect confirming Casimir's calculations [6]. The static effect was measured numerous times following Lamoreaux first attempt [7].

More recently, experimental validations of the dynamical Casimir effect and the Casimir torque have been confirmed which allows direct observational evidence of the vacuum fluctuations and removing all the remaining confusion about the origin of the Casimir effect [32]. The dynamical Casimir effect was first conceptualized in 1970 by [33] where two mirrors are oscillated at near relativistic speed to effectively pump the vacuum fluctuations and extract real photons out of it. In 2011, the first experimental study reported the extraction of microwave photons in a technique involving a modified SQUID confirming the dynamical Casimir effect [8]. The beginning of the abstract reporting on the experimental results in *Nature* makes an impactful statement

One of the most surprising predictions of modern quantum theory is that the vacuum of space is not empty. In fact, quantum theory predicts that it teems with virtual particles flitting in and out of existence. While initially a curiosity, it was quickly realized that these vacuum fluctuations had measurable consequences, for instance producing the Lamb shift of atomic spectra and modifying the magnetic moment for the electron. **Wilson, 2011** [8]

The effect was confirmed by a second group in 2013 [34] then again in 2019 [35].

These results open the door to using the Casimir torque as a micro- or nanoscale actuation mechanism, which would be relevant for a range of technologies, including microelectromechanical systems and liquid crystals. [...] The van der Waals and Casimir effects both result from the same mechanism (quantum and thermal fluctuations), although historically they were derived from different physical pictures. **Somers, 2018** [36]

All the experimental results presented above are gathered in Table 1 validating experimentally the existence of electromagnetic vacuum fluctuations as well as establishing them as the source of creation and annihilation of pairs of particles.

ZPE-based Effect	Theoretical Prediction/Explanation	Experimental Validation	Additional Reference
Black Body radiation	Planck (1900-1912) [14]	Kirchhoff (1860) [37]	Milonni (1993 ) [5]
Photoelectric effect	Einstein (1905) [38]	Millikan (1916) [39]	Lehnert (2014 ) [40]
Spontaneous Photon Emission	Einstein (1916)	N/A	Dirac (1927) [11]
Lamb Shift	Bethe (1947) [41]	Lamb-Rutherford (1947) [9]	
Casimir Effect	Casimir (1948) [42]	Lamoreaux (1997) [6]	Bordag (2001) [7]
Casimir Torque	Casimir (1948)	Somers (2018) [36]	
Dynamical Casimir Effect	Moore(1970) [33]	Wilson(2011) [8]	Dodonov (2020) [32]
Hawking Radiation-Unruh Effect	Hawking-Zeldovich (1972-1973) - Unruh(1976)		
Electron-Positron pair creation	Dirac (1928) [43]	Anderson (1932) [12]	
Schwinger effect	Sauter (1931) [27] - Schwinger (1951) [28]	National Graphene Institute - Geim (2022) [13]	
Vacuum Birefringence	Heisenberg - Euler (1936)	STAR experiment (2021) - IXPE (2022) [10]	
Breit-Wheeler Effect	Breit-Wheeler (1934) [44]	Pike <i>et al</i> (2014) [45]	
Higgs mechanism	Anderson (1962) [46]	LHC (2013)	

Table 1: List of physical effects based on the ZPE with the theoretical prediction or post-experiment explanation and corresponding experimental validation.

## 2 ZPE density consequences on spacetime, mass definition and matter stability.

In this section, we will review the consequences of ZPE on the spacetime structure and how it is related to the definitions of mass in the standard model.

### 2.1 Calculation of ZPE density

Now that we have built the theoretical origin of the ZPE and confirmed its existence by the current experimental validations, we derive the total vacuum energy density. ZPE density only arises in coherent space (see Appendix B) and results from the sum of all elementary spherical harmonic oscillators with ground state energy  $E_0(\omega)$  on all possible modes  $\omega$  of the fields (See derivation in Appendix D). For three dimensional spherical oscillators (as mentioned above being resonant cavities as in Figure 1), the ground state energy of the rotational oscillations is given by

$$E_0(\omega) = \frac{3}{2}\hbar\omega \quad (2.1)$$

and the vacuum energy density for a continuous mode distribution is

$$\begin{aligned} \rho_{vac} &= \frac{1}{V} \sum_{\omega} n(\omega) E_0(\omega) = \frac{2\pi}{V} \int_0^{\omega_{max}} E_0(\omega) dn(\omega) \\ &= \frac{3\hbar}{2\pi c^3} \int_0^{\omega_{max}} \omega^3 d\omega = \frac{3\hbar}{8\pi c^3} \omega_{max}^4 \end{aligned} \quad (2.2)$$

where  $dn(\omega)$  corresponds to the number of modes between  $\omega$  and  $\omega + d\omega$  in a volume  $V$ . If an infinity of possible modes is allowed, *i.e.*  $\omega_{max} \rightarrow \infty$ , the vacuum density  $\rho_{vac}$  would diverge. Yet, the frequencies  $\omega$

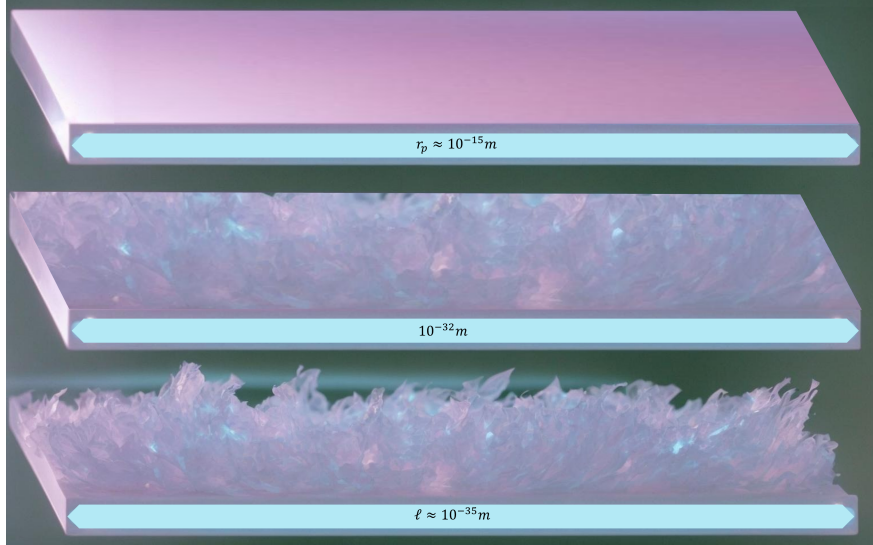


Figure 2: Illustration of the quantum foam where the energy level is directly related to the observation scale at which one measures. A flat surface at the charge radius  $r_p \sim 10^{-15} \text{ m}$  can result from intense and turbulent vacuum fluctuations at the Planck scale  $\ell \sim 10^{-35} \text{ m}$ .

correspond to a wavelength scale at which the observations are made. Thus, the vacuum energy divergence occurs when an infinite amount of scales is considered underlying the possible fractal nature of spacetime at the quantum scale, which is found as well at the cosmological scale at black hole singularity. Furthermore, spacetime vacuum that appears flat at a large scale is in fact extremely energetic and fluctuating at the small scale of the quantum world (Figure 2).

Since Einstein's general relativity equations demonstrate that all energy sources will geometrize spacetime, and curved spacetime geometry is gravity, the tremendous amount of vacuum fluctuation energy of the zero-point energy density should result in a highly curved (multiply-connected) spacetime geometry and strong gravitational action which is apparently not observed at our scale as demonstrated by Wheeler in his paper *Quantum Geometrodynamics* [25]. However, the continuous process of creation-annihilation creating continuous distortion of spacetime occurs at very short distance scales. Quantum fluctuations of the geometry of spacetime are so violent that the usual picture of a smooth spacetime with a metric on it breaks down. Instead, one should visualize spacetime as a 'quantum foam', a superposition of all possible topologies which only looks smooth and placid on large enough length scales (Figure 2). Wheeler compared the quantum foam with the surface of an ocean. Very far from the surface, it can be considered as perfectly flat such that no energy is observed. Zooming in however, at the scale where the waves can be observed, an energy can be measured. If we continue to zoom in, we will see the wave breaking and even the foam forming at the surface. All those scales of observation can be associated to an energy, that is to say in the case of spacetime, a mass.

## 2.2 Natural cut-off at the quantum scale

By simple relationship analysis between general relativity and quantum mechanics, we can heuristically find a minimum wavelength scale, where the regularization cut-off is set by the spacetime dynamics combined with the Heisenberg uncertainty principle emerging from ZPE which provides a minimal value for the angular momentum of an extremal spacetime vortex of momentum  $p$  and energy  $Mc^2$  with a radius  $R$

$$\Delta x \Delta p \geq \frac{\hbar}{2} \quad (2.3)$$

where  $\Delta x = R$  represents the vortex radius and  $\Delta p$  the relativistic momentum flow ( $\Delta p \approx Mc$ ). Thus, the minimal angular momentum  $\Gamma_m = MRc$  is  $\hbar/2$  and it obeys the condition :

$$MR = \frac{\hbar}{2c} \quad (2.4)$$

Such structure would form in the spacetime metric producing quantum foam at the critical Schwarzschild limit. Thus,

$$\frac{M}{R} = \frac{c^2}{2G} \quad (2.5)$$

By resolving the two conditions Equation (2.4) and Equation (2.5) from quantum mechanics and general relativity, we obtain the cut-off condition equivalent to the unifying energy occurring at the Planck scale:

$$R = \sqrt{\frac{\hbar G}{c^3}} = \ell \quad (2.6)$$

$$M = \frac{1}{2} \sqrt{\frac{\hbar c}{G}} = \frac{m_\ell}{2} \quad (2.7)$$

with  $m_\ell$  and  $\ell$  the Planck mass and length respectively. Therefore, Planck length and Planck mass define a minimum scale in the spacetime structure, typically chosen as a limit as well at the center of black holes singularity or in the big bang cosmology.

Although this computation is heuristic in nature, it has the virtue to clearly illustrate that the only non-arbitrary units, or natural units, of the Planck scale (where forces are unified), are congruent with the Schwarzschild solution to Einstein field equations, defining an elementary spacetime pixel due to vacuum fluctuations and producing quantum foam.

This cut-off and its associated quantum foam was further demonstrated by Wheeler (in [25]) who calculated the characteristic length scale at which spacetime metric fluctuations can be observed as a response of vacuum electromagnetic fluctuations. Wheeler analyzed the phase of the Feynman-Huygens equation for a field that combines an Einstein-Hilbert action and an electromagnetic free field such that the exponent phase is described by

$$\frac{S_H}{\hbar} \sim \int [(c^3/8\pi\hbar)(\partial g/\partial x)^2 + (1/8\pi\hbar c\mu_0)(\partial A/\partial x)^2] (-g)^{1/2} d^4x \quad (2.8)$$

where  $S_H$  is the Einstein-Hilbert action with a potential vector  $A$  and  $g_{\mu\nu}$  the spacetime metrics. For a typical region of space  $L^4$ , the phase variation  $\delta\varphi$  in the path integral formulation due to alterations of the metrics component  $\delta g$  and electromagnetic fluctuations of the potential vector  $\delta A$  can be written as [25]

$$\delta\varphi = \delta S_H/\hbar \sim (c^3/\hbar G)L^2(\delta g)^2 + (1/\hbar c\mu_0)L^2(\delta A)^2 \quad (2.9)$$

where the phases are defined as

$$\delta\varphi_g = \frac{c^3 L^2 (\delta g)^2}{\hbar G} : \text{gravitational phase} \quad (2.10)$$

$$\delta\varphi_{em} = \frac{L^2 (\delta A)^2}{\hbar c \mu_0} : \text{electromagnetic phase} \quad (2.11)$$

The field variations of such region of space contribute to the path histories when phase variations are small enough to create constructive interferences ( $\delta\varphi \sim 1$ ), this corresponds to the minimal value for the field action  $\delta S_H = \hbar/2$ . Also, according to Einstein's field equations, in a vacuum, spacetime curvature will result from the electromagnetic field energy density given by

$$R_{\mu\nu} - \frac{1}{2}Rg_{\mu\nu} = \frac{8\pi G}{c^4}T_{\mu\nu} \quad (2.12)$$

Considering small variations of the metric  $\delta g$ , Einstein's equations for the metric component reduces to

$$\frac{\delta g^2}{L^2} \sim \frac{G}{c^4} \frac{B^2}{\mu_0} \quad (2.13)$$

The electromagnetic energy density  $\mathcal{E} = \frac{B^2}{\mu_0}$  for small variations of the potential vector  $\delta A$  is given by

$$\begin{aligned} B &\sim \frac{\delta A}{L} \\ \mathcal{E} &= \frac{B^2}{\mu_0} \sim \frac{1}{\mu_0 L^2} \delta A^2 \end{aligned} \quad (2.14)$$

Thus, the spacetime curvature resulting from electromagnetic vacuum fluctuations induces a metric variation  $\delta g$  defined by

$$\frac{\delta g^2}{L^2} \sim \frac{G}{c^4} \frac{B^2}{\mu_0} \sim \frac{G}{c^4 L^2 \mu_0} \delta A^2 \quad (2.15)$$

$$\delta g^2 \sim \frac{G}{c^4} \frac{\delta A^2}{\mu_0}$$

(2.16)

Therefore, the electromagnetic and gravitational phases are of the same order  $\delta\varphi_g \sim \delta\varphi_{em} \sim 1$

$$\frac{L^2}{\ell^2}(\delta g)^2 \sim \frac{L^2}{\hbar c \mu_0} (\delta A)^2 \sim 1 \quad (2.17)$$

As a result, the typical metric and electromagnetic field energy density fluctuations are

$$\delta g \sim \frac{\ell}{L} \quad (2.18)$$

$$\delta \mathcal{E} \sim \frac{\delta A^2}{\mu_0 L^2} \sim \frac{\hbar c}{L^4} \quad (2.19)$$

The metric reaches a maximum fluctuations when  $\delta g \sim 1$  (see Appendix E). Then, the characteristic length  $L$  of the metric fluctuations is of the order of the Planck length

$$L \sim \ell \quad (2.20)$$

Similarly, the energy of the electromagnetic field oscillators at the Planck length scale is of the order of the Planck mass:

$$M \sim \frac{\delta \mathcal{E} \ell^3}{c^2} = m_\ell \quad (2.21)$$

Wheeler's investigation of electromagnetic vacuum fluctuations inducing a gravitational response, led to what he coined quantum foam. He found that these fluctuations have qualitative and quantitative consequences at distances in the order of the Planck length,  $\ell$ , where the metric fluctuations  $\delta g$  are coherent enough. Therefore, the spacetime curvature fluctuations due to vacuum fluctuations give birth to creation and annihilation of virtual wormholes described by Wheeler having a charge of the order of the Planck charge  $q_\ell = \sqrt{4\pi\epsilon_0\hbar c} \sim 12e$ , a mass of the order of the Planck mass,  $m_\ell$ , and a typical energy  $E = m_\ell c^2 \sim \rho_{vac} \ell^3$  associated to ZPE ( $\rho_{vac}$ ). Then Wheeler investigated the possibility that the mass and charge of elementary particles could be described from a quantum geometrodynamical point of view. This would mean that mass and charge of elementary particles, such as the electron, would result from a collective and coherent disturbance of vacuum fluctuations associated with the metric and gravitational fluctuations generated by the creation-annihilation of Planck size micro-wormholes.

### 2.3 Consequences of the Planck length cut-off

Here, we have used two different approaches to describe the relationship between electromagnetic vacuum fluctuations and spacetime curvature resulting in a natural cut-off value of the spacetime structure at the quantum scale. Similar to these results already in 1967 prominent physicist Andrei Sakharov explored the possibility of a microscopic foundation to gravitation from quantum vacuum fluctuations that he coined 'the metric elasticity of space', where he utilized the Planck length cut-off as well and found an equivalence between the electromagnetic fluctuations of the vacuum and the gravitational constant  $G$  [47]

$$G = \frac{c^3}{16\pi\hbar\mathcal{C} \int kdk} = \frac{2c^3\ell^2}{16\pi\mathcal{C}\hbar} \quad (2.22)$$

with  $\mathcal{C} = \frac{1}{8\pi}$  is a geometrical constant of the order of unity and  $\int kdk$  is the sum of all reachable modes of the vacuum electromagnetic fluctuations. Considering the Planck length cut-off, according to Sakharov's definition, the gravitational force results directly from the intensity of the fluctuations in the quantum foam [48]<sup>11</sup>.

Returning to Equation (2.2)  $\rho_{vac} = \frac{3\hbar}{8\pi c^3} \omega_{max}^4$  and renormalizing with an oscillator of characteristic diameter of the order of the Planck length  $\ell$ , we obtain a cut-off pulsation

$$\omega_{max} = \frac{2\pi c}{2\pi \frac{\ell}{2}} = \frac{2c}{\ell} \quad (2.23)$$

and a finite vacuum energy density expressed as

$$\boxed{\rho_{vac} = \frac{6}{\pi} \frac{c^7}{G^2 \hbar} \approx 8.90 \times 10^{113} \text{ J.m}^{-3}} \quad (2.24)$$

Although this is typically the value given for the quantum vacuum energy density (or ZPE) which is extremely high (in the order of Planck density), one must keep in mind that the system energy density is directly related to the correlation time  $\tau$  (see Appendix B) delineating and characterizing a coherent state of constructive interferences which corresponds to a characteristic scale defined by the system effective time. Thus, it's possible to compute the system energy density  $\rho$  by considering the electromagnetic vacuum fluctuations correlation time  $\tau$  such as (see Appendix B)

$$\rho(\tau) = \epsilon_0 \left\langle \vec{E}(\vec{r}, t), \vec{E}(\vec{r}, t + \tau) \right\rangle \approx \frac{6}{\pi} \frac{\hbar c}{(c\tau)^4} = \rho_{vac} \left( \frac{t_\ell}{\tau} \right)^4 \quad (2.25)$$

where  $t_\ell$  is the Planck time.

Therefore, when a characteristic time  $\tau = t_\ell$ , we clearly find  $\rho_{vac}$  giving a deeper meaning to the cut-off wavelength and being directly related to the coherency of the vacuum fluctuations defining the energy levels of the system. Remarkably, when we consider a significant change of scale, and we implement the characteristic time of the proton  $\tau_p$  defined by

$$\tau_p = \frac{r_p}{c} \approx 2.8 \times 10^{-24} \text{ s} \quad (2.26)$$

where  $r_p$  is the proton rms charge radius, which is as well consistent with the characteristic time of the strong nuclear force typically given by the  $\rho$  meson lifetime ( $4 \times 10^{-24} \text{ s}$ ), we obtain the energy density  $\rho_p$  of that scale from  $\rho_{vac}$  considering the creation and annihilation cycle reducing by a factor of 2

$$\boxed{\rho_p = \frac{\rho_{vac}}{2} \left( \frac{t_\ell}{\tau_p} \right)^4 = \frac{3}{\pi} \frac{\hbar c}{r_p^4} \approx 6.05 \times 10^{34} \text{ J/m}^3} \quad (2.27)$$

Thus, the corresponding energy  $\mathcal{E}_p$  for that scale resulting from the coherent behavior of the quantum vacuum fluctuations in the volume of a proton is

$$\mathcal{E}_p = \frac{4}{3} \pi r_p^3 \times \rho_p = 4 \frac{\hbar c}{r_p} = 938 \text{ MeV} \quad (2.28)$$

---

<sup>11</sup>p.427-428

Considering that the rest mass of the proton is known to be  $938 \text{ MeV.c}^{-2}$ , our computation precisely finds the energy equivalent of a proton from a coherent structure of vacuum fluctuations at that scale. In this non-trivial result, we find a clear origin of the mass-energy emerging from quantum vacuum fluctuations at the Planck scale, through a decoherence or screening mechanism that generates the proton rest mass.

From a completely different approach of an external point of view, this correlation time  $\tau_p$  can be as well thought of as the characteristic time of a resonant cavity of a length  $r_p = c\tau_p$  generating a Casimir force equivalent to an energy gradient by eliminating the short wavelength of vacuum fluctuations. Thus, considering the proton as a resonant cavity, we sum all the cavity resonant modes  $\lambda$  and obtain once again equation (2.27)

$$\rho_p = -\frac{12}{\pi} \int_{r_p}^{\infty} \frac{\hbar c}{\lambda^5} d\lambda = \frac{3 \hbar c}{\pi r_p^4} \quad (2.29)$$

Here our computation finds a precise value (limited by the precision on the proton radius) for the hadronic mass and clearly suggests, as we will demonstrate further, that the nuclear confining force analogous to the Casimir effect, and the mass, arise from the ZPE quantum vacuum fluctuations dynamics. In fact, we note that the binding pressure force arising from a Casimir resonant cavity at a characteristic distance of a proton is on the same order of magnitude as the strong interaction [49, 50]

$$F_{\text{Casimir}} \sim \rho_p \times A_p \approx 10^4 \text{ N} \quad (2.30)$$

The current standard mechanism to define the source of the rest mass of the proton usually requires the strong nuclear force contribution to make up the deficiency of the Higgs mechanism, which only predicts  $\sim 1$  to  $5\%$  of the proton mass [3, 4]. Furthermore, the fundamental origin of confinement and the residual nuclear force (or strong force) given by quantum chromodynamics (QCD) has no analytical solution or origin. Therefore, the origin of mass for matter in our universe remains an open issue, notwithstanding dark matter and dark energy which is thought to be  $\sim 95\%$  of the mass-energy of the universe.

The screening and reduction of energy from ZPE to the proton rest mass-energy scale and the nuclear force, or residual strong force, was first explored in [51] and [52] by consideration of a semi-permeable horizon surface defining the mechanism of decoherence of the vacuum energy density  $\rho_{\text{vac}}$  to produce the mass-energy of particles and forces.

We note that our result, from the correlation functions, relates the charge radius of the proton not only to the rest mass, but as well to the reduced Compton wavelength  $\lambda_p = \frac{\hbar}{m_p c}$  giving a direct relationship between the charge radius and  $\lambda_p$  given as

$$\boxed{\mathcal{E}_p = 4 \frac{\hbar c}{r_p} = m_p c^2 = \frac{\hbar c}{\lambda_p}} \Rightarrow \boxed{\lambda_p = \frac{r_p}{4}} \quad (2.31)$$

This emerging characteristic length  $\lambda_p$  was utilized by Hideki Yukawa for the effective radius of residual strong force [53] and will become significant in the screening process explored in sections 3 & 4.

### 3 Spacetime lattice and the Holographic Mass Solution

#### 3.1 Electromagnetic Harmonic Oscillators

From the correlation functions, defining the coherence of a symmetrically ordered system resulting in the energy at different scales depending on the correlation time  $\tau$  and following Wheeler's quantum foam bubbles approach, we compute utilizing Equation (2.21) and Equation (2.24) the geometry of the elementary oscillator or voxel of the field  $\rho_{vac}$  having the electromagnetic field energy of the order of the Planck mass  $m_\ell$ . Thus, for a volume  $V$  filled by  $N$  space filling voxels of mass-energy  $m_\ell$  having an equivalent density  $\rho_{vac}$  we find

$$\rho_{vac} = \frac{6}{\pi} \frac{c^7}{G^2 \hbar} = \frac{Nm_\ell c^2}{V} \quad (3.1)$$

where the number of oscillators in the volume  $V$  is given by

$$N = \frac{V}{V_0} \quad (3.2)$$

where  $V_0$  is the elementary oscillator volume. Combining the two equations, it results

$$\frac{6}{\pi} \frac{c^5}{G^2 \hbar} = \frac{m_\ell}{V_0} \quad (3.3)$$

and solving it for the voxel's volume  $V_0$ , we get

$$\begin{aligned} V_0 &= \frac{\pi}{6} \frac{m_\ell G^2 \hbar}{c^5} \\ &= \frac{\pi}{6} \left( \frac{\hbar G}{c^3} \right)^{3/2} \\ &= \frac{4\pi}{3} \left( \frac{\ell}{2} \right)^3 \end{aligned} \quad (3.4)$$

Therefore, the voxel appears to be a spherical foam bubble of radius  $\frac{\ell}{2}$  and mass-energy  $m_\ell$ . It is consistent with the initial description of a spherical cavity given as the harmonic oscillator (Figure 1). Furthermore, the space filling nature of the computation must be kept in the context of a dynamical foam of spherical bubbles appearing and disappearing, as creation and annihilation cycles, resulting in a space-filling symmetry. These Planck spherical bubble *units*, or spherical quantum harmonic oscillators, constitute the fabric of spacetime structure at the Planck scale and have been previously termed as Planck Spherical Units (PSU) [52]. The PSU is the elementary oscillator of ground state energy  $E_0 = \frac{1}{2}\hbar\omega$ .

We compute the PSU characteristic time  $\tau_{psu}$  at their ground energy level  $E_0$  from the PSU resonant frequency

$$\tau_{psu} = \omega_{psu}^{-1} \quad (3.5)$$

By comparing the PSU mass-energy  $m_\ell$  with its ground state energy at the resonant frequency  $\omega_{psu}$  we obtain the equation

$$\frac{1}{2}\hbar\omega_{psu} = m_\ell c^2 \quad (3.6)$$

And, solving it for the resonant frequency, we get

$$\omega_{psu} = \frac{2m_\ell c^2}{\hbar} = \frac{2c}{\ell} \quad (3.7)$$

Thus, the fluctuation time of a PSU cycle is of the order of the Planck time with each foam bubble following a creation and annihilation cycle of period  $2\tau_{psu} = t_\ell$

$$\tau_{psu} = \frac{\ell}{2c} = \frac{t_\ell}{2} \quad (3.8)$$

where  $t_\ell = \frac{\ell}{c}$  is the Planck time.

PSU as elementary constituents of spacetime form a plasma-like superfluid structure flowing at all scales. At the quantum scale, this flow is found as the ZPE fluctuations  $\rho_{vac}$ , which is consistent with Dirac's analysis of the potential vector  $A_\mu$  resulting in a velocity of an underlying medium [54, 55]. In his study on spontaneous emission [11], Dirac also commented on the zero-point energy : "The light-quantum has the peculiarity that it apparently ceases to exist when it is in one of its stationary states, namely, the zero state." When PSU are in the ZPE state, their energy is below the quantum of energy  $E_0 < \hbar\omega$  such that we cannot see them. Once they become coherent and adopt a collective movement they start to create an energy flow that we call mass. We identify this energy flow as a Planck plasma with phase transitions generating boundaries resulting in energy screening.

### 3.2 The quantum spacetime structure

The Planck plasma flow of PSU can be compared to a quark-gluon plasma (QGP), where at high energy densities quarks and gluons are freed of their strong attraction for one another [56]. QGP is described as a highly coherent fluid and was experimentally discovered in high energy colliders [57, 58]. As the coherence decreases mass and strong force appear, such that all the structured matter is supposed to derive from this early-universe cooling process. Similarly, but in our case occurring in a time independent manner (stationary process) and true at all scales, the Planck plasma energy density  $\rho_{vac}$  undergoes phase transitions resulting in a reduction of coherence and thus of energy. The resulting screening process is described here with a focus on the proton scale, which is the source of baryonic mass in the universe and a specific emphasis on the relationship between its nuclear force and gravity. Although our earlier computation of the correlation functions clearly indicated a direct relationship between quantum vacuum fluctuations  $\rho_{vac}$  and the production of the rest mass at the proton effective time scale (Equation (2.27)), further investigations must occur to understand clearly the mechanism in which the  $\rho_{vac}$  energy density transits from its highly coherent phase within the proton core (as in the coherent QGP) to a less coherent phase generating the rest mass energy.

The first noteworthy observation using Equation (2.28) is that the relationship between the rest mass density and the vacuum density naturally generates the well-known gravitational coupling constant  $\alpha_g = \frac{Gm_p^2}{\hbar c} = 16 \left(\frac{\ell}{r_p}\right)^2$  relating the nuclear force strength to the apparently weak gravitational Newtonian force [59]

$$\frac{\rho_p}{\rho_{vac}} = \frac{1}{2} \left(\frac{\ell}{r_p}\right)^4 = \frac{\alpha_g^2}{512} = \frac{\alpha_g^2}{8^3} \quad (3.9)$$

This emergence of  $\alpha_g$  in the decoherence process and energy reduction gives us a first inkling of a scaling relationship between the nuclear force energy potential and the gravitational potential. This scaling factor was noticed and investigated by others including B.J. Carr and M.J. Rees [60]. The factor  $8^3$  that appears as well implies that there must be a geometric parameter to be considered in the screening mechanism of the electromagnetic vacuum fluctuations.

The quantity  $\frac{\ell}{r_p}$  given in radii is a reduction of the physical representation of a system which must be defined in three dimensions as volumes enclosed in surfaces. To understand the deeper mechanism underlying the

screening of  $\rho_{vac}$  one must consider the surface capacity in terms of vacuum fluctuations or information to radiate the enclosed energy as in the Bekenstein entropy bound, which implies that the information of a physical system is encoded on its surface where the upper bound entropy is reached at the black hole condition [61].

Every it, derives from bits **John Archibald Wheeler, 1989** [62]

We compute, in our case, the screening coefficient  $\eta_p$  of a proton surface composed of fluctuating PSU shielding the available interior vacuum energy  $\rho_{vac}$ . Thus, the number of oscillating PSU cross-section  $\pi \left(\frac{\ell}{2}\right)^2$  tilling the proton surface  $A_p = 4\pi r_p^2$  gives the screening coefficient  $\eta_p$

$$\eta_p = \frac{4\pi r_p^2}{\pi \left(\frac{\ell}{2}\right)^2} = 16 \left(\frac{r_p}{\ell}\right)^2 = \frac{256}{\alpha_g} \quad (3.10)$$

Equations (3.9) and (3.10) suggest that there are two phase transitions or screening surfaces on the order of  $\eta_p = 256\alpha_g^{-1}$  to reduce from  $\rho_{vac}$  to the rest mass-energy density of the proton (Figure 3). From the result of the correlation functions computation (Equation (2.28)), we identify the first screening surface  $\eta_\lambda$  being at the reduced Compton wavelength  $\lambda_p$  and the second screening surface  $\eta_p$  at the proton charge radius  $r_p$ .

$$\rho_p = \frac{\rho_{vac}}{2} \left(\frac{\ell}{r_p}\right)^4 = \rho_{vac} \frac{1}{\eta_\lambda} \times \frac{8}{\eta_p} \quad (3.11)$$

We then define  $\mathcal{R}$  as the number of PSU in the volume of the system representing the internal energy of the quantum vacuum fluctuations  $\rho_{vac}$  available in the volume enclosed by the screening surface  $\eta$

$$\mathcal{R} = \frac{\rho_{vac} V}{m_\ell c^2} = \frac{\frac{4}{3}\pi r^3}{\frac{4}{3}\pi \left(\frac{\ell}{2}\right)^3} = 8 \left(\frac{r}{\ell}\right)^3 \quad (3.12)$$

Therefore, the geometric mechanism resulting in the rest mass of the proton from the vacuum fluctuations as in Equation (2.28) can be written as

$$m_p = \frac{\rho_p V_p}{c^2} = 8 \frac{\mathcal{R}_p}{\eta_\lambda \times \eta_p} m_\ell \quad (3.13)$$

The above results give us a direct, remarkable, and non-trivial geometric relationship between the decoherence of the electromagnetic quantum vacuum fluctuations  $\rho_{vac}$ , the origin of mass, and scales of the forces involved between the gravitational potential and the nuclear force. Furthermore, it provides an insight into the geometric mechanism that produces a reduction of energy at the proton scale and, as we will see later, at various scales of baryonic matter and at the cosmological scale. Unlike the QED scheme which reduces the mass of particles from an infinite 'bare' mass using vacuum fluctuations, we identify the vacuum fluctuations as the source of mass that is shielded to produce the observed mass-energy density. Examining Equation (3.13) we find that the production of mass for the proton, which constitutes most of the mass in the universe, from the ZPE  $\rho_{vac}$  requires two surface screenings by the surface vacuum fluctuations  $\eta_\lambda$  and  $\eta_p$  enclosing the volumes  $\mathcal{R}_\lambda$  and  $\mathcal{R}_p$ , respectively. We now investigate the physical meaning of these surfaces and their relationship to spacetime dynamics.

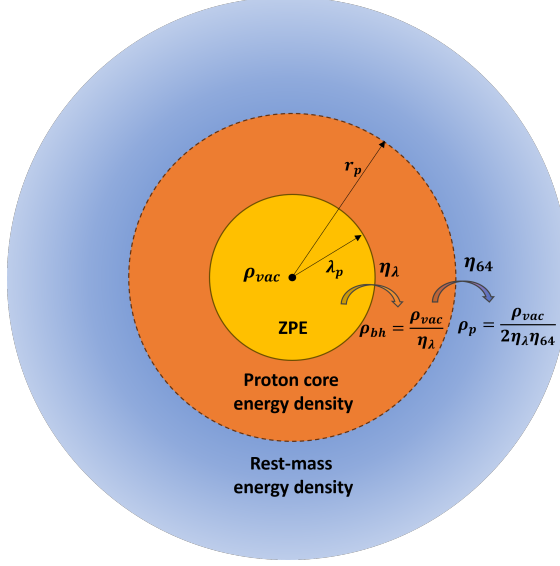


Figure 3: Schematic representation of the screening processes producing the rest mass from the quantum vacuum fluctuations  $\rho_{vac}$  which is associated to two screening surfaces: the first screening at the Compton wavelength  $\lambda_p = \frac{r_p}{4}$  and the second screening at the proton charge radius  $r_p$  resulting in a first energy density  $\rho_{bh} = \frac{\rho_{vac}}{\eta_\lambda}$  and the rest mass energy density  $\rho_p = \frac{\rho_{vac}}{2\eta_\lambda\eta_{64}}$ , respectively.

### 3.3 First screening and Einstein Field Equations

Examining the relationship of the electromagnetic vacuum fluctuations between the volume  $\mathcal{R}$  and the surface screening  $\eta$  we discover a relationship to cosmology and find a direct and non-trivial path to general relativity, or spacetime. To deeper understand the screening mechanism principle we ignore, for now, the relationship to the proton from which the surface to volume information/energy ratio was found and we generalize it to see if it relates to any fundamental physical principle. We find

$$M = \frac{\rho_{vac}V}{\eta c^2} = \frac{\mathcal{R}}{\eta}m_\ell \quad (3.14)$$

Computing the mass  $M$  we obtain

$$M = \frac{\mathcal{R}}{\eta}m_\ell = \frac{\frac{4}{3}\pi r^3}{\frac{4}{3}\pi (\frac{\ell}{2})^3} \times \frac{\pi (\frac{\ell}{2})^2}{4\pi r^2} \times m_\ell = \frac{r}{2\ell}m_\ell \quad (3.15)$$

and thus

$$M = \frac{r}{2\ell}m_\ell = \frac{r}{2} \sqrt{\frac{c^3}{\hbar G}} \sqrt{\frac{\hbar c}{G}} = \frac{rc^2}{2G} \quad (3.16)$$

$$M = \frac{\mathcal{R}}{\eta}m_\ell = \frac{rc^2}{2G}$$

(3.17)

where Equation(3.16) corresponds to the first exact solution to Einstein Field Equations (EFE), *i.e.*, the Schwarzschild solution  $r_s = \frac{2GM}{c^2}$ . Thus, we find a clear relationship between the first screening and the fundamental physics of spacetime producing a gravitational horizon. This is another remarkable result considering that only vacuum fluctuations at the quantum scales were considered with a surface screening mechanism that now clearly relates to the semi-permeable structure of the event horizon of a black hole given by the Schwarzschild solution  $r_s$ . Furthermore, this gives us a profound insight on the structure and geometry of the surface horizon of a black hole congruent with the holographic principle and Bekenstein black

hole entropy conjecture [63], where here the surface pixelization by PSU  $\eta$  represents the information energy encoded on the surface utilized in the Hawking-Bekenstein entropy of a black hole

$$S = \frac{k_B A}{4\ell^2} = k_B \frac{\pi}{16} \eta \quad (3.18)$$

with  $k_B$  the Boltzmann constant. From this expression of Hawking entropy which eventually leads to Hawking temperature of a black hole, the surface pixelization  $\eta$  can be seen as a *surface information*. In our case, from quantum mechanics and geometric consideration alone, we obtain a fundamental result of general relativity. This has significant implications in the unification of physics as this result relates gravitational curvature to the source of the stress energy tensor being quantum vacuum fluctuations. As such, the Schwarzschild metric  $ds$  typically given as (in  $(-, +, +, +)$  convention)

$$ds^2 = - \left(1 - \frac{2GM}{rc^2}\right) c^2 dt^2 + \left(1 - \frac{2GM}{rc^2}\right)^{-1} dr^2 + r^2 d\Omega^2 \quad (3.19)$$

is an analytical solution of EFE

$$R_{\mu\nu} - \frac{1}{2} R g_{\mu\nu} + \Lambda g_{\mu\nu} = \frac{8\pi G}{c^4} T_{\mu\nu} \quad (3.20)$$

where  $R_{\mu\nu}$  is the Ricci tensor,  $R$  the Ricci scalar,  $g_{\mu\nu}$  is the metric tensor,  $T_{\mu\nu}$  is the stress-energy tensor and  $\Lambda$  is the cosmological constant.

Not so well known is the fact that from our derivation the Schwarzschild metric can be written from the mechanics of mass production emerging from vacuum fluctuations as

$$ds^2 = - \left(1 - \frac{2\ell}{r} \frac{M}{m_\ell}\right) c^2 dt^2 + \left(1 - \frac{2\ell}{r} \frac{M}{m_\ell}\right)^{-1} dr^2 + r^2 d\Omega^2 \quad (3.21)$$

As a result, the Planck units and the zero-point energy  $\rho_{vac}$  are the natural normalization factors of general relativity in Einstein field equations

$$\left(R_{\mu\nu} - \frac{1}{2} R g_{\mu\nu} + \Lambda g_{\mu\nu}\right) \ell^2 = 48 \frac{T_{\mu\nu}}{\rho_{vac}} \quad (3.22)$$

Keeping in mind that EFE are fluid dynamic equations, it is appropriate to study them in their dimensionless form in order to evaluate the amplitude of the mechanics involved. This dimensionless version sets the Planck scale as the fundamental scale and ZPE density  $\rho_{vac}$  corresponds to the energy density required to obtain a spacetime curvature on the order of the Planck length  $R_{\mu\nu} - \frac{1}{2} R g_{\mu\nu} + \Lambda g_{\mu\nu} \sim \frac{1}{\ell^2}$ , which is consistent with the cut-off found earlier (see section 2).

Beyond the fact that the Planck units generate a compact and elegant formulation of the metric, a deep mechanical meaning emerges from this treatment. Equations (3.14), (3.15), (3.16), (3.22) provide a direct relationship between a black hole mass (thus the stress-energy tensor in EFE) and quantum vacuum fluctuations  $\rho_{vac}$ , scaled through a purely geometric parameter

$$\frac{\mathcal{R}}{\eta} = \Phi^{-1} \quad (3.23)$$

given by [64] as the holographic ratio. This brings further insights into the relationship between the quantum electromagnetic field, the origin of mass-energy required in the Einstein stress-energy tensor and the gravitational spacetime manifold curvature at any scale. We find that the black hole mass  $M$ , responsible for intense gravitational force and spacetime curvature, originates from a certain level of decoherence in electromagnetic vacuum fluctuations screened by the information entropy stored at its surface  $\eta$ .

This supports Sakharov's approach of 1967 discussed earlier, that electromagnetic vacuum fluctuations can be the source of the spacetime elasticity generating the gravitational constant (or vice versa) which could have led the way to a profound understanding of the unification of forces and the source of mass. As well,

in 1973, an autodidact physicist, who had a great influence in standard physical theory, Yakov Zeldovich, demonstrated based on previous work from Gertsenshtein [65] and Landau [66] that electromagnetic waves under specific conditions are converted into gravitational waves [67]. Not so well-known as well is the fact that Karl Schwarzschild at the same period of his calculation of the exterior solution for EFE published the same year (in 1916) an interior solution considering a perfect incompressible fluid to compute spacetime dynamics in the interior of the black hole [68].

Contrary to the classical approach, where one would expect the black hole formation to be the result of an accretion of infalling material to a critical limit, our result demonstrates that black hole formation is the result of a natural spacetime behavior emerging from a state of coherency of the collective quantum vacuum fluctuation oscillators in a region of space at different scales. The mechanism that defines these states of coherency are related to the angular momentum of an oscillator, as described by Max Planck originally. The coupling of the oscillators produces collective behaviors or a quantum vortex in a turbulent flow of the spacetime manifold in a region of space generating what we observe as a black hole. The details of such fluid dynamics, that we coined a *Planck Plasma flow* and their relationship to the electromagnetic field and the gravitational manifold are beyond the scope of this manuscript and will be appearing in a much larger publication (work in progress) permitting their derivation.

We note that this mechanism of black hole formation from coherent modes of vacuum energy may explain the latest observations of the James Webb Space Telescope finding supermassive black holes at  $z > 5$  at the very early universe where star formation and accretion would not have been possible to produce them [69, 70].

The first screening solution not only changes the concept of black hole formation and its source of mass but as well the QFT perspective in which the vacuum fluctuations are responsible for the bare mass shielding by virtual particles. To be clear, the vacuum fluctuations are the source of mass and the shielding is due to the dynamical properties of the PSU flow which is similar to quark-gluon plasma at thermal and chemical equilibrium with their color charge and force. As we have just seen, this shielding is related to the horizon surface of a black hole. Furthermore, this mechanism is in accordance with Stephen Hawking analysis of the early universe formation finding that “a sufficient concentration of electromagnetic radiation can cause gravitational collapse” forming primordial and elementary black holes of Planck length and Compton wavelength size [71].

### 3.3.1 First screening applied at the proton scale

Following this line of thoughts of primordial black holes, we apply the screening mechanism  $\eta_\lambda$  at the reduced Compton radius  $\lambda_p = \frac{\hbar}{m_p c}$  and obtain an analog to the ‘undressed’ mass or ‘bare’ mass of the proton  $M_p$

$$M_p = \frac{\rho_{vac}}{\eta_\lambda c^2} V_p \quad (3.24)$$

where  $V_p$  is the proton volume at the reduced Compton radius and the pixelization screening surface  $\eta_\lambda$  is defined as

$$\eta_\lambda = \frac{4\pi\lambda_p^2}{\pi\left(\frac{\ell}{2}\right)^2} = 16\left(\frac{\lambda_p}{\ell}\right)^2 \quad (3.25)$$

This concept of black hole proton was partially presented by one of us examining what would be the energy level requirement provided by the quantum vacuum fluctuations energy density at the proton scale to obey the Schwarzschild solution. In these early publications first attempts of reconciling the strong confining force with gravity was heuristically demonstrated [51, 64]. Combining Equations (3.9), (3.13) and (3.24) we find the gravitational coupling constant  $\alpha_g$

$$\frac{m_p}{2M_p} = \alpha_g \approx 5.91 \times 10^{-39} \quad (3.26)$$

This strongly suggests that the relationship between a black hole proton core and its rest mass correctly describes the force gradient between the confining color force or strong force given by the coupling constant

$\alpha_s$ , which is typically given in the order of unity, and the gravitational force given by  $\alpha_g$ . This will be treated in details in section 4.

Although the concept of particles being black holes or at least 'hosting' singularities at their core might be shocking at first encounter, one may consider that the density of quantum vacuum fluctuations in a region of space largely exceed the value required to obey the Schwarzschild condition of a black hole and thus it follows that the Planck length obeys that very condition (notwithstanding a factor of 2 denser which will be discussed in the next section)  $\frac{2Gm_\ell}{c^2} = 2\ell$  (Equation (3.28)). Furthermore, throughout the modern history of physics, significant literature explored this possibility as a result of the quantum structure of spacetime, for instance with the event of general relativity predictions of Einstein-Rosen bridges [72] where Einstein and Rosen considered that in order for spacetime to retain continuity, particles would have to be bridges between region of space later coined wormholes by Wheeler in 1957 [73]. In 1935, Einstein and Rosen stated when describing the bridges between two Minkowski sheets "These solutions involve the mathematical representation of physical space by a space of two identical sheets, a particle being represented by a "bridge" connecting these sheets. [...] here is a possibility for a general relativistic theory of matter which is logically completely satisfying and which contains no new hypothetical elements." This idea of a complete geometric approach applying at the quantum scale was furthered by Wheeler's *Geometrodynamics* and his explorations of Quantum Foam [25]. In his papers on *Geometrodynamics*, Wheeler defined particles as a collective coherence of Planck size wormholes establishing a continuity between the Planck scale spacetime dynamics and particle creation. Eventually, with the event of string theory the concept of particles being related to black hole physics became prominent resulting in Leonard Susskind stating "One of the deepest lessons that we have learned over the past decade is that there is no fundamental difference between elementary particles and black holes" [74].

### 3.3.2 First screening applied at the Planck scale

We now apply the first screening mechanism at the Planck scale to investigate the size of the smallest black hole of mass  $m_\ell$  created from vacuum fluctuations  $\rho_{vac}$ . By considering the Planck mass and our discussion above, equation (3.14) yields

$$M = \frac{\rho_{vac}V}{\eta_\ell c^2} = m_\ell \quad (3.27)$$

we then deduce the Schwarzschild radius of this smallest blackhole

$$r_s = 2\ell \quad (3.28)$$

In terms of the holographic mass solution for a black hole of radius  $2\ell$ , we find

$$M = \frac{\mathcal{R}}{\eta} m_\ell = \frac{64}{64} m_\ell = m_\ell \quad (3.29)$$

Therefore, and remarkably, where general relativity meets the Planck scale the initial micro black hole pixel emerging from vacuum fluctuations is found to have an equivalence information structure between volume to surface ratio of 64 PSU in the volume and 64 PSU on the surface, such that the information ratio  $\Phi$  is in the order of unity generating a first scale voxel screening with a mass of the order of the Planck mass  $m_\ell$ . This elementary black hole, which we coined kernel-64, has a volume 64 times larger than a PSU, which illustrates the screening mechanism and suggests dynamical processes and geometric relationships that occur in the Planck plasma flow within black hole structure. This kernel-64 is considered as a primary state of PSU organization. Previously, similar micro-black holes constructs were referred to *instantons* by Carr and Rees in [60] stating that "space may be thought of as being filled with virtual black holes of this size. Such instantons have an important role in quantum gravity theory". Also envisioned by Wheeler in his treatment of quantum geometrodynamics was a geon (a Gravitational Electromagnetic Entity) described as a self-gravitating particle [75–77] curving spacetime inducing the encapsulation of the energy radiation to produce a particle.

### 3.4 Second screening for the proton rest mass

One can consider the continuing aggregation of self-gravitating islands of PSU oscillators forming scale relationships in the Planck plasma as it undergoes phase transitions from the event horizon into a less coherent phase carrying less energy. This mechanism of energy screening can be represented as self-gravitating oscillators curving spacetime to encapsulate the internal energy reducing the available effective energy of the decoherent phases. Between the Compton wavelength horizon and the charge radius surface, the Planck plasma flow transits from single PSU to kernel-64 aggregates. This aggregation mechanism gives us a deeper understanding of the second screening resulting in the proton rest mass (Equation(2.28)): while the first screening  $\eta$  at the horizon has a mesh of characteristic wavelength  $\frac{\ell}{2}$ , the second screening has a larger wavelength  $2\ell$  letting through not single PSU but instead larger aggregates of 64 PSU carrying a mass-energy information of  $m_\ell$  (Figure 6). Therefore, the surface information capacity reduces to

$$\eta_{64} = \frac{4\pi r_p^2}{\pi(2\ell)^2} = \frac{1}{16} \frac{4\pi r_p^2}{\pi (\frac{\ell}{2})^2} = \frac{\eta_p}{16} \quad (3.30)$$

Thus, from Equation(3.13), the holographic mass solution expression for the rest mass can be decomposed to describe the two screenings,  $\eta_\lambda$  and  $\eta_{64}$  carrying an information packet  $m_\ell$  giving

$$m_p = 8 \frac{\mathcal{R}_p}{\eta_\lambda \times \eta_p} m_\ell = \frac{1}{2} \frac{\mathcal{R}_p}{\eta_\lambda \times \eta_{64}} m_\ell = 2\Phi_p m_\ell \quad (3.31)$$

In terms of energy density, the proton rest mass density is expressed from the ZPE  $\rho_{vac}$  as

$$\rho_p = \frac{1}{2} \frac{\rho_{vac}}{\eta_\lambda \times \eta_{64}} \quad (3.32)$$

As a result, we find that this encapsulation mechanism describes the second screening correctly predicting the rest mass of the proton as emerging from the change of state of the grain structure of the vacuum fluctuations. The factor  $\frac{1}{2}$  earlier associated with the pairs creation and annihilation process in the correlation functions becomes clearer as it may be related to a Hawking type radiation of the internal black hole source identified as the first screening, where one particle falls inwards and the other is radiated outwards. We now calculate this energy.

### 3.5 Hawking radiation

In 1973, S.W. Hawking conceived, inspired by the work of J. Bekenstein on black holes entropy [63] as well as the work of Y. Zel'dovich and A. Starobinsky [78], that vacuum fluctuations in the surrounding strong gravitational field of a black hole undergo radiation as the dynamics of 'virtual' pairs of particles creation and annihilation cycles occur in proximity of the event horizon, resulting in one particle of the pair falling into the black hole, and the other one being radiated as a 'real' particle. This process would slowly evaporate the black hole energy as the 'negative' energy of the infalling particle would extract energy from the black hole [79]. While this picture has been widely accepted the details of the mechanisms relating the quantum vacuum fluctuations and the horizon of a black hole are still shrouded in some obscurity. One of them is the *trans-planckian problem* where field modes very near to the horizon of a black hole can have frequencies that transcend the Planck time scale generating divergent energy density similar to ZPE. In our case, the spacetime dynamics combined with the Heisenberg uncertainty principle limits the range of frequencies characterizing our scale (see section 2.2), as well the phase of the Feynman-Huygens equation for a field that combines an Einstein-Hilbert action, and an electromagnetic free field defines the Planck length as the scale at which metric fluctuations are on the order of unity. Therefore, assuming the Hawking radiation mechanism is somewhat correct, although it has not been directly verified experimentally, it would stand to reason that if our solution to the origin of mass from  $\rho_{vac}$  undergoes a first decoherence phase transition at a black hole condition that one could calculate the Hawking radiation resulting from it at the proton scale.

Applying Stefan-Boltzmann law for black body radiation, the radiated energy of the core proton black hole between  $\lambda_p$  and  $r_p$  at the charge radius surface  $\mathcal{A} = 4\pi r_p^2$ , over the characteristic time  $\tau_p = \frac{r_p}{c}$  is

$$\mathcal{E} = \sigma T_\lambda^4 \mathcal{A} \tau_p \quad (3.33)$$

where  $T_\lambda$  is the Hawking temperature generated by the Compton horizon  $\lambda_p$ . Considering the space between the Compton horizon and the charge radius surface filled with vacuum fluctuations acting as a superfluid, we have an isothermal process between these two surfaces. Hawking utilized Bekenstein's work on black hole entropy to derive the Schwarzschild black hole entropy of radius  $r_s$  as a pixelization of the black hole cross-section with Planck squares of size  $\ell^2$

$$S = k_B \frac{A}{4\ell^2} = k_B \frac{\pi r_s^2}{\ell^2} \quad (3.34)$$

and the corresponding Hawking temperature as a function of the Planck temperature  $T_\ell = \sqrt{\frac{\hbar c^5}{G k_B^2}}$  and the entropy  $S$

$$T(r_s) = \frac{\hbar c}{4\pi r_s k_B} = \frac{T_\ell}{4\sqrt{\pi}} \sqrt{\frac{k_B}{S}} \quad (3.35)$$

Clearly nature does not tile in squares  $\ell^2$  and a more natural representation would be the cross section of a sphere as seen earlier in the second screening surface  $\eta_{64}$ , pixelized by kernel-64 of radius  $2\ell$ . Tiling the Compton cross-section  $A_\lambda/4$  we find

$$S = k_B \mathcal{C} \frac{A_\lambda/4}{\pi(2\ell)^2} = k_B \mathcal{C} \frac{\lambda_p^2}{(2\ell)^2} \quad (3.36)$$

where  $\mathcal{C}$  is the surface compacity characterizing the kernel-64 circle packing of the Compton cross-section. We find the Hawking temperature

$$T_\lambda = \frac{1}{4\sqrt{\mathcal{C}\pi}} \frac{2\ell}{\lambda_p} T_\ell = \sqrt{\frac{4\pi}{\mathcal{C}}} \frac{\hbar c}{4\pi k_B \lambda_p} = \sqrt{\frac{4\pi}{\mathcal{C}}} T(\lambda_p) \quad (3.37)$$

Thus, the radiated energy expression simplifies to

$$\begin{aligned} \mathcal{E} &= \sigma A_p T_\lambda^4 \tau_p \\ &= \frac{\pi^2 k_B^4}{60 \hbar^3 c^2} \left( \sqrt{\frac{4\pi}{\mathcal{C}}} \frac{\hbar c}{4\pi k_B \lambda_p} \right)^4 4\pi r_p^2 \frac{r_p}{c} \\ &= \frac{4\pi}{15\mathcal{C}^2} \frac{4\hbar c}{r_p} \\ &= \frac{4\pi}{15\mathcal{C}^2} \mathcal{E}_p \end{aligned} \quad (3.38)$$

Therefore, the Hawking radiation energy transferred by black body radiation mechanism resulting from vacuum fluctuations pair production at the Compton horizon  $\lambda_p$  (recall that black body radiation is intimately linked with ZPE) and diffusing to the charge radius surface  $r_p$  generates the proton rest mass-energy with consideration of a geometric correction factor on the entropy of the system. This indicates that the second screening process  $\eta_{64}$  can also be described by a Hawking-like radiation mechanism transferring the energy from the semi-permeable black hole horizon  $\eta_\lambda$  resulting in the proton rest-mass energy (Figure 4). We find the packing compacity is

$$\mathcal{C} = \sqrt{\frac{4\pi}{15}} \sim 0.915 \quad (3.39)$$

which is within 0.009 or less than 1% higher than the compacity for hexagonal circle packing  $\mathcal{C} = \frac{\pi}{2\sqrt{3}} \sim 0.906$ , or

$$\boxed{\mathcal{E} = \sigma T_\lambda^4 \mathcal{A} \tau_p \sim m_p c^2} \quad (3.40)$$

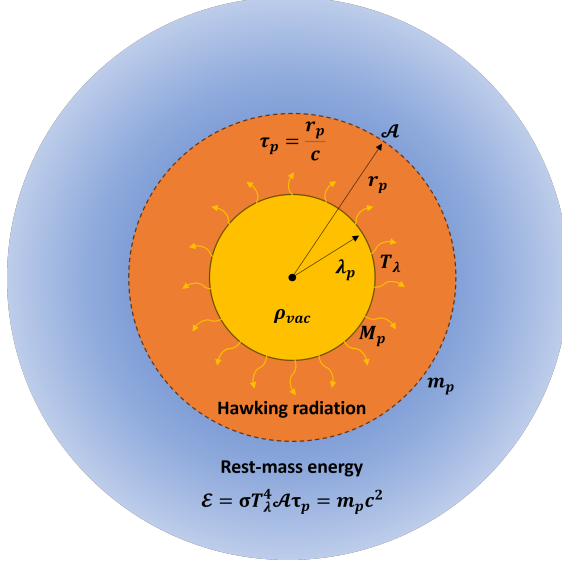


Figure 4: Schematic representation of the Hawking radiation of the first screening energy density. The black hole mass  $M_p$  from one screening of the quantum vacuum fluctuations  $\rho_{vac}$  by  $\eta_\lambda$  at the reduced Compton wavelength  $\lambda_p$  radiates the rest mass  $m_p$  at the proton charge radius  $r_p$ .

### 3.6 Hawking evaporation

In the initial study of Hawking temperature [80], Bardeen, Carter and Hawking considered axisymmetric solutions containing a perfect fluid with circular flow around a central black hole. We have shown from the above solution that a black hole, whether a proton or a cosmological black hole, emerges from the flow of the quantum vacuum fluctuations, or Planck plasma  $\rho_{vac}$ , undergoing a phase transition or shielding at the semi-permeable horizon which is a mechanism that can be associated with the process utilized by Hawking to obtain his black hole evaporation construct [81]. We now calculate the life expectancy of such black hole irradiating mass-energy undergoing Hawking radiation considering the internal source term  $\rho_{vac}$  or total interior energy  $\mathcal{R}m_\ell c^2$ . At a size  $r$ , a black hole interior vacuum energy is

$$E_{int} = \mathcal{R}m_\ell c^2 = \frac{8r^3}{\ell^3}m_\ell c^2 \quad (3.41)$$

A variation of energy  $dE$  is therefore associated to a reduction of PSU and black hole interior size  $dr$  following

$$dE = 24m_\ell c^2 \frac{r^2}{\ell^3} dr \quad (3.42)$$

Over a time  $dt$  the system radiates the energy  $dE$

$$dE = -\sigma T(r, t)^4 \mathcal{A}(r, t) dt = -\frac{4\pi}{15C^2} \frac{4\hbar c^2}{r^2} dt \quad (3.43)$$

which corresponds to system size variation  $dr$  over a time  $dt$

$$dE = 24m_\ell c^2 \frac{r^2}{\ell^3} dr = -\frac{4\pi}{15C^2} \frac{4\hbar c^2}{r^2} dt \quad (3.44)$$

we can thus evaluate the evaporation time of a proton black hole as

$$t_{evap} = \int_0^{t_{evap}} dt = \frac{-\gamma}{c} \int_{\lambda_p}^0 \frac{5r^4}{\ell^4} dr = \frac{\gamma \lambda_p^5}{c \ell^4} \approx 7.64 \times 10^{44} \text{ years} \quad (3.45)$$

where  $\gamma = \frac{9}{2\pi} C^2$  is a numerical factor.

Equation (3.45) can similarly be used to evaluate the reduction  $\delta$  in proton black hole radius since the estimated beginning of the universe  $t_u = 13.7 \times 10^9$  years

$$t_u = \int_0^{t_u} dt = \frac{-\gamma}{c} \int_{\lambda_p+\delta}^{\lambda_p} \frac{5r^4}{\ell^4} dr = \frac{\gamma((\lambda_p + \delta)^5 - \lambda_p^5)}{c\ell^4} \underset{\frac{\delta}{\lambda_p} \ll 1}{\sim} \frac{5\gamma\lambda_p^4\delta}{c\ell^4} \quad (3.46)$$

then

$$\delta = \frac{t_u c \ell^4}{5\gamma\lambda_p^4} \approx 7.54 \times 10^{-52} \text{ m} \quad (3.47)$$

We find a proton black hole lifetime that is extremely long, on the order of  $10^{35}$  billion years, making proton energy structure perfectly stable over very long periods of time. Furthermore, since the estimated beginning of the universe, the proton would have decayed an infinitesimal energy consistent with an extremely stable particle over time. No measurable variations to the mass or the radius would be observable within the short span of the contemporaneous age-estimate of the universe.

### 3.7 Proton charge radius

A precise knowledge of charge radii is important for benchmarking *ab initio* nuclear theory.

**Antognini *et al.*, 2022** [82]

The proton charge radius  $r_p$  is a fundamental quantity in particle physics for the precise determination of fundamental constants such as the Rydberg constant ( $R_\infty$ ). It also challenges our understanding of the Standard Model for precise calculations of the energy levels and transition energies of the hydrogen atom, for example, the Lamb shift [82, 83] (Figure 5). The proton radius is generally defined by the slope of the proton charge form factor  $G_p^E$  at zero momentum transfer  $t$  which is determined in the non-perturbative regime of the strong interaction [84]

$$r_p^2 = 6 \frac{dG_p^E(t)}{dt} \Big|_{t=0} \quad (3.48)$$

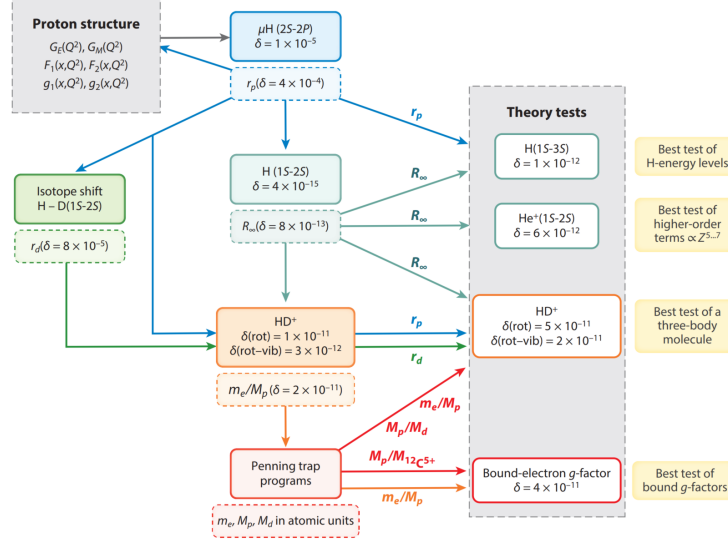


Figure 5: Implication of the proton charge radius measurements in the Standard Model (extracted from [82]).

Historically, two experimental methods are used to determine proton charge radius : the hydrogen spectroscopy (H spec, also called electron Lamb shift) and the electron-proton scattering (e-p scat) [84–86]. Before 2010, most measurements of the two methods had large uncertainties and indicated a mean proton radius situated

around the Codata 2010 value  $\sim 0.87$  fm considered as the 'large' radius. With the advent of the muonic hydrogen spectroscopy ( $\mu$ H spec), consisting of replacing the electron by the heavier muon, the measurement of the proton charge radius became more precise and provided a 'small' radius of  $r_p = 0.84184(67)$  fm. The 4% difference between the large and small proton radius was at that time known as the proton radius 'puzzle' as no-one could decide which value was the right value [84].

From the Holographic rest mass solution of the proton (Equation(3.31)), Haramein successfully predicted in 2012 the proton charge radius from the experimental data of the proton mass [87], confirming the  $\mu$ H spec of the small proton radius in 2013 [88]. Equation (3.31) relates the proton rest mass to its charge radius which allows prediction of the proton charge radius, given the rest mass and *vice versa*. Table 2 presents the latest Codata values for proton rest mass and radius ( $m_p$  and  $r_p$ ) as well as the corresponding prediction from the Holographic mass solution ( $m_p^{th}$  and  $r_p^{th}$ ). The charge radius of the proton is directly related to its mass and reduced Compton wavelength  $\lambda_p$  :

$$r_p = 4\ell \frac{m_\ell}{m_p} = \frac{4\hbar}{m_p c} = 4\lambda_p. \quad (3.49)$$

This early success of the holographic mass solution relies on the fact that the ZPE is at the center of the solution. In QFT and QCD theory, the ZPE is mostly ignored by restructuring the Lagrangian terms. The Holographic mass solution is built on the Vacuum electromagnetic fluctuations and evaluates its effect based on the phase coherence of the system. In fact, by describing the equation relating the proton mass and its charge radius, the Holographic mass solution is able to predict the exact value constituting a validation of the Holographic mass solution as an appropriate nuclear theory. This example highlights also the difficulties of QCD theory to predict new values as the coupling constants, QCD free parameters, required a fitting with experimental data and making predictions extremely difficult.

$r_p$ (experimental Codata 2018)	$m_p$ (experimental Codata 2018)	$r_p^{th}$
0.8414(19) fm	1.67262192369(51) $\times 10^{-27}$ kg	0.84132150851 fm

Table 2: Latest Codata 2018 values for the proton rest mass  $m_p$  and proton charge radius  $r_p$ , and the predicted values for the holographic proton charge radius  $r_p^{th}$ .

From 2017, new experimental data for the e-p scat measurements with smaller momentum transfer were refining the proton radius in favor of the small proton radius [85, 86]. These new insights motivated a review of the analysis of the model used to derive the proton radius on the old measurements dataset. The new models included the electromagnetic vacuum fluctuations by combining time-like measurements, such as the creation of nucleon and anti-nucleon creation in electron-positron annihilation and its reverse reaction, with the space-like measurements [89]. Surprisingly, the use of the ZPE in the re-analyses of the old electron-proton scattering data shifted the 'large' proton radius to the 'small' proton radius, which ended the proton radius 'puzzle' and set its latest Codata 2018 value of  $r_p = 0.8414(19)$  fm (already predicted by Haramein in 2012 [87]).

## 4 Nuclear force and residual strong force

### 4.1 Planck Force: the ground state

Frank Wilczek, along with David Gross and David Politzer, Nobel prize laureates in physics for their formulation of asymptotic freedom, utilized running coupling constants to characterize quarks and gluons interactions. While our screening mechanism describes a decoherence from  $\rho_{vac}$  energy density to produce the Schwarzschild condition (first screening  $\eta_\lambda$ ) and the radiation of the rest-mass (second screening  $\eta_{64}$ ), Wilczek *et al.* described an anti-screening process due to the Yang–Mills vacuum, that Gross described as an analog to paramagnetism, and where “QCD is asymptotically free because the anti-screening of the gluons overcomes the screening due to the quarks” [90]. This was instrumental to save quantum field theory inconsistencies where forces were formally infinite at very short distance (interestingly as in a spacetime singularities), and now resulting in the creation of a ‘color’ confinement where quarks and gluons cannot be isolated. The quarks pair are thought to ‘snap’ the gluon tube that confines them when the separation energy level reaches the quark-antiquark pair energy creation, such a separating force is estimated to be reached at  $\sim 10^4$  N [50].

In 1999, Wilczek utilizing this formalism of force interactions and his work on asymptotic freedom recovered an expression for the proton rest-mass that he associated with the anti-screening function of the forces coupling constant  $\alpha_{unified}$  at the ‘unification’ energy of the Planck mass [91]

$$m_p \sim \exp(-k/\alpha_{unified}) m_\ell \quad (4.1)$$

where  $\alpha_{unified} \approx \frac{1}{25}$  is the common value of the strong, electromagnetic and weak couplings when they unify, and  $k = \frac{11}{2\pi}$  is a calculable numerical factor that characterizes the anti-screening. This treatment is a good order approximation for the proton rest-mass and is similar in nature with the holographic mass solution given in Equation (3.31). Thus, considering Wilczek anti-screening approach and our screening mechanism described earlier, we find a relationship with the holographic ratio of the proton  $\Phi_p$

$$\exp(-k/\alpha_{unified}) \approx \frac{1}{2} \frac{\mathcal{R}_p}{\eta_\lambda \times \eta_{64}} = 2\Phi_p \quad (4.2)$$

In 2001, Wilczek, resulting from his exploration of the running coupling constants and the hadronic of mass, states “If we accept that  $G_N$  (the gravitational constant  $G$ ) is a primary quantity, together with  $\hbar$  and  $c$ , then the enigma of  $N$ ’s smallness (the gravitational coupling constant  $\alpha_g$ ) looks quite different. We see that the question it poses is not, ‘Why is gravity so feeble?’ but rather, ‘Why is the proton’s mass so small?’ for in natural (Planck) units, the strength of gravity simply is what it is, a primary quantity, while the proton’s mass is the tiny number  $\sqrt{N}$ .” [2] While Wilczek’s comment is absolutely correct and well placed, from our result we find that the ‘tiny’ rest mass of the proton is in fact the result of a much larger energy density  $\rho_{vac}$  expressing a strong gravitational region and force at the first screening  $\eta_\lambda$  which is reduced by a significantly large number at the second screening of the rest mass  $\eta_{64} \sim 10^{39}$ . Here, Wilczek is pointing to Dirac large number hypothesis introducing  $N$ , a large dimensionless number, that seems to emerge as a natural ratio in the universe linking length, mass and forces at different scales explored by others as well [60, 92, 93]. This large number  $N$ , or  $\alpha_g$ , commonly defined from the proton rest mass is given by

$$\alpha_g = \frac{m_p}{2M_p} = \frac{Gm_p^2}{\hbar c} \approx 5.91 \times 10^{-39} \quad (4.3)$$

where  $M_p$  is the vacuum energy density after the first screening at  $\lambda_p$ . Rearranging this equation Rees and later Wilczek found the scaling relationship between the proton rest mass and the Planck mass. Later, Haramein gave a deeper understanding of the source of mass through vacuum fluctuations coherent collective behavior resulting in the holographic mass solution

$$m_p = \sqrt{\alpha_g} m_\ell = 2\Phi_p m_\ell \quad (4.4)$$

Therefore,

$$\alpha_g = 4\Phi_p^2 \quad (4.5)$$

where  $\Phi_p = \frac{\eta_p}{\mathcal{R}_p}$ . Proton rest mass is key because it provides a complementary pattern for the screening mechanism as well as a complementary understanding of the gravitational coupling constant as the ratio between the proton energy  $m_p c^2$  and the vacuum energy

$$\mathcal{R}_p m_p c^2 = 2\eta_\lambda \eta_{64} m_p c^2 = 128\alpha_g^{-2} m_p c^2 \quad (4.6)$$

Considering that the gravitational coupling constant  $\alpha_g$  is typically thought of as the force ratio between gravity and the strong force [59], this result strongly suggests that not only the rest-mass energy emerges from the black hole Hawking radiations, or the second screening, but that the strong force is directly related to the curvature of spacetime at the hadronic scale by the energy density of the proton black hole phase. To find the origin of the forces, and in consideration of our result, we calculate the gravitational force between two PSU interacting in the Planck Plasma vacuum fluctuations

$$\frac{Gm_\ell^2}{(2\frac{\ell}{2})^2} = \frac{c^4}{G} = F_\ell \approx 1.21 \times 10^{44} \text{ N}$$

(4.7)

As would be expected we find the Planck force as the Planck scale is thought to be the unification energy where forces ratio become on the order of unity. As such we can think of the Planck force as the ground state of force generating forces at different scales.

## 4.2 General relativity under pressure

In general relativity, it is usual to consider a perfect fluid in the stress energy tensor to model an idealized distribution of matter and to obtain an exact solution to Einstein field equations as in the Schwarzschild interior solution [68], the interior of a star and Friedman-Lemaître-Robertson-Walker (FLRW) model of an homogeneous and isotropic universe [48]. In such spacetime fluid solution we can relate the energy density  $\rho$  to the fluid pressure  $P(\rho)$  through an equation of state given here as

$$P(\rho) = \frac{2}{3}\rho \quad (4.8)$$

Consequently, the Planck force  $F_\ell$  corresponds to the vacuum pressure force experienced by PSU in the Planck Plasma flow

$$F_\ell = P_{vac} \sigma_{PSU} = \frac{2}{3}\rho_{vac} \pi \left(\frac{\ell}{2}\right)^2 \quad (4.9)$$

where  $\sigma_{PSU}$  represents the PSU cross-section typically used as the effective surface in fluid dynamics for a solid sphere in a turbulent flow. More generally, from equation (3.22), it follows that Einstein proportionality constant  $\kappa$  (Einstein gravitational constant) for the stress energy tensor on the right-hand side of the field equations can be expressed as a function of the Planck force resulting from a vacuum pressure  $P_{vac} = \frac{2}{3}\rho_{vac}$  as the source of curvature

$$R_{\mu\nu} - \frac{1}{2}Rg_{\mu\nu} + \Lambda g_{\mu\nu} = \frac{48}{\rho_{vac}\ell^2}T_{\mu\nu} \quad (4.10)$$

or

$$R_{\mu\nu} - \frac{1}{2}Rg_{\mu\nu} + \Lambda g_{\mu\nu} = \frac{8\pi}{F_\ell}T_{\mu\nu} \quad (4.11)$$

Here Einstein gravitational constant which is typically thought as a proportionality factor clearly displays a physical meaning, deeply rooted at the quantum scale, as the ground state pressure of the Planck plasma flow where

$$\kappa = \frac{48}{\rho_{vac}\ell^2} = \frac{32}{P_{vac}\ell^2} = \frac{8\pi}{F_\ell} \quad (4.12)$$

From this analysis of  $\kappa$ , the Planck force can be seen as a pressure force exerted by the vacuum fluctuations pressure  $P_{vac}$  on the Planck plasma flow and is the reference ground state force from which nucleation at

the Planck scale occurs, *i.e.* as in Wheeler's quantum foam [25] describing this pressure as an analog to the surface tension of a bubble [94]. This pressure corresponds to the force required to generate a surface horizon at the Planck scale against the rigid elasticity of spacetime. Thus, one can estimate the stress-energy tensor trace  $T_\mu^\mu$  at the horizon and find a direct analogy between the surface tension in Young-Laplace equation in 4D-spacetime  $\gamma = \kappa^{-1} \ell^{-2} = \frac{\rho_{vac}}{48}$  [95] and the stress-energy tensor structuring the spacetime manifold

$$\frac{1}{r^2} = \kappa T_\mu^\mu = 3\kappa\rho \quad (4.13)$$

Using the equation of state we recognize a Young-Laplace type equation for our horizon hyper-surface curvature

$$P = 2\gamma \frac{\ell^2}{r^2} = \frac{F_\ell}{4\pi r_s^2} \quad (4.14)$$

where  $\frac{\ell^2}{r^2} \sim \eta^{-1}$  is the spacetime curvature and our screening surface confining the electromagnetic vacuum fluctuations within the region of space and screening the energy and force experienced outside that region. Consequently and more generally, in order to form a stable Schwarzschild bubble black hole in spacetime at any scale  $r_s$ , the black hole energy density repulsive pressure required to compensate the spacetime elasticity  $F_\ell$  is given by

$$F = \frac{2}{3}\rho S = \frac{2}{3}\frac{Mc^2}{\frac{4}{3}\pi r_s^3}4\pi r_s^2 = F_\ell \quad (4.15)$$

As demonstrated above considering  $\rho_{vac}$  to be the source of mass and  $F_\ell$  resulting from the flow of  $\rho_{vac}$  curving spacetime, we evaluate the mechanism in which the strong color confinement, the nuclear force and eventually the gravitational force, responsible for black hole formation, originate from the same screening process of the ground state force  $F_\ell$  by generalizing the Equation (4.9) for any phases energy densities  $\rho$  (see Figure 6) as

$$F(\rho) = \frac{2}{3}\rho \pi \left(\frac{\ell}{2}\right)^2 \quad (4.16)$$

### 4.3 Planck Force first screening

From Equation (4.16) we can now evaluate the pressure force produced by the vacuum density at scales in which measurements can be observed, *i.e.* at the baryonic scale of the proton where the color confinement force and the residual strong force have been probed through scattering experiments and quark-gluon plasma dynamics. Therefore, we apply our first screening mechanism  $\frac{\rho_{vac}}{\eta_\lambda}$  to compute the numerical value and verify that the mechanism is consistent with mass-energy production from  $\rho_{vac}$ . We find the value of the confining force  $F_s$  as

$$F_s = \frac{2}{3}\frac{\rho_{vac}}{\eta_\lambda} \pi \left(\frac{\ell}{2}\right)^2 = \frac{F_\ell}{\eta_\lambda} \approx 4.54 \times 10^4 \text{N} \quad (4.17)$$

This value is in agreement with the recent and astonishing measurements which succeed in measuring the interior pressure force of the proton and experienced by quarks [49, 50]. This is as well commonly associated with the confining force strength expected at the horizon of the proton corresponding to the snapping of 'gluon tubes' resulting in quark-antiquarks pair creations [96]. In general, the quark-antiquarks binding energy is in the range of 89 MeV – 332 MeV depending on the quark flavor considered [97], and the characteristic distance of the force corresponding to where the gluon string breaking takes place between  $q\bar{q}$  pair is just above  $d_{q\bar{q}} \sim 1.2$  fm [98]. The resulting estimated force strength is

$$F_{q\bar{q}} \sim \frac{\Lambda}{d_{q\bar{q}}} \approx 1.19 \times 10^4 \text{ N} - 4.43 \times 10^4 \text{ N} \quad (4.18)$$

Remarkably, utilizing the same mechanism of screening of quantum vacuum fluctuations  $\rho_{vac}$ , which led to the Schwarzschild solution, applied to the ground state force  $F_\ell$ , we find that the force exerted equivalent to the mass energy in that region of space corresponds to the confinement force at the horizon expected for the structure of the proton quark-antiquark confinement [99]. This force can be interpreted in two different ways: the gravitational force between two PSU separated by a characteristic distance of the proton charge radius  $r_p$

$$F_s = \frac{F_\ell}{\eta_\lambda} = \frac{Gm_\ell^2}{r_p^2} \quad (4.19)$$

or as the proton black hole mass  $M_p$  gravitationally binding the proton rest mass energy at  $r_p$  surrounding the  $\lambda_p$  horizon

$$F_s = \frac{2GM_p m_p}{r_p^2} \quad (4.20)$$

This derivation demonstrates that both the origin of the gravitational force and color force is the result of the Planck force  $F_\ell$  and the Planck energy flow pressure  $P_{vac}$  generating a highly curved space within the proton interior. Thereafter, the quark-gluon formalism, where the gluon flux tubes force snaps to generate quark-antiquark pairs out of the vacuum fluctuations and generate confinement, is related to the electromagnetic Planck plasma pressure of the quantum vacuum that we have demonstrated to be the origin of mass and now confinement. The formalism defining this fluid dynamics and quantum vortex structure will be published in a larger manuscript, however it is important to note that it is related in principle and mechanism to recent advancements in lattice QCD utilizing center vortices to describe confinement/deconfinement contributions of the gluon strings [100, 101].

It is also important to note that there is no classical nor clear definition for the strong force in the standard model. The strong force emerged from the observation that two positively charged protons should not be able to bind due to electrostatic repulsion. QCD built up a complex formalism attempting to describe the strong force based on quark-antiquark interactions. The QCD model describes these interactions as the sum of the exchange energy of gluons between slow charmed quarks with the linear confinement potential and the spin-dependent interaction that can occur between charm-anticharm pairs. QCD theory uses 9 free parameters through the six quarks masses and the three running coupling constants for each quark flavor. QCD is a non-analytical theory where any computation of the QCD Lagrangian requires many approximations, while our solution is analytical and grounded in the fundamental physics of both spacetime and quantum mechanics.

#### 4.4 Second screening of the Planck force

We further investigate the result of the second mass-energy screening by computing the pressure within the rest-mass energy density region  $\rho_p = \frac{1}{2} \frac{\rho_{vac}}{\eta_\lambda \times \eta_{64}}$  utilizing the equation of state (4.8)

$$P_p = \frac{2}{3} \frac{\rho_{vac}}{\eta_\lambda \times 2\eta_{64}} = 4 \times 10^{34} \text{ Pa} \quad (4.21)$$

This pressure is in agreement with the recent and astonishing measurements which succeeded in measuring the pressure experienced by quarks in the proton interior and is found to be in the order of magnitude of the pressure within the core of a neutron star [49, 50, 102] or a stellar-size black hole. We then compute the resulting pressure force experienced by the fluid particle, namely the kernel-64, of the proton external region (see Figure 6)

$$F_g = \frac{2}{3} \frac{\rho_{vac}}{\eta_\lambda \times 2\eta_{64}} \pi (2\ell)^2 = \frac{8F_\ell}{\eta_\lambda \eta_{64}} = \frac{\alpha_g^2}{32} F_\ell = \frac{2Gm_p^2}{(2r_p)^2} \quad (4.22)$$

which corresponds to the gravitational force between two contiguous protons. We note that the force ratio between the strong force  $F_s$  and the Newtonian gravitational force  $F_g$  corresponds to the well-known gravitational coupling constant  $\alpha_g$  describing the weakness of the gravitational interaction between two rest-mass protons

$$\frac{F_g}{F_s} = \frac{m_p}{4M_p} = \frac{\alpha_g}{2} \quad (4.23)$$

This is consistent with the analysis of the black hole proton mass-energy producing the strong color confinement occurring at the first screening of  $\rho_{vac}$  and the weakness of the rest mass resulting from the second screening

$$\frac{F_g}{F_s} = \frac{m_p}{4M_p} = \frac{8\eta_\lambda}{\eta_\lambda\eta_{64}} = \frac{8}{\eta_{64}} \quad (4.24)$$

$F_\ell = \frac{Gm_\ell^2}{(2\frac{\ell}{2})^2} = \frac{\hbar c}{\ell^2}$	$\approx 1.17 \times 10^{44} N$	PSU interaction: Planck force
$F_s = \frac{F_\ell}{\eta_\lambda} = \frac{Gm_\ell^2}{r_p^2} = \frac{\hbar c}{r_p^2} = \frac{\alpha_g}{16} F_\ell$	$\approx 4.54 \times 10^4 N$	Q̄Q Interaction: Color confinement force
$F_g = 2 \frac{Gm_p^2}{(2r_p)^2} = \frac{8F_s}{\eta_{64}} = \frac{8F_\ell}{\eta_\lambda\eta_{64}} = \frac{\alpha_g^2}{32} F_\ell$	$\approx 1.32 \times 10^{-34} N$	Newtonian Gravitational force

Table 3: Summary of the Planck force screening resulting in the color confinement force  $F_s$  and the Newtonian gravitational force  $F_g$

We demonstrate that the high intensity of the nuclear confinement forces is derived from quantum vacuum fluctuations  $\rho_{vac}$  curving spacetime and underlying the fundamental nature of forces at the quantum scale as pressure in the Planck plasma flow eventually resulting in the Newtonian gravitational force ( $F_g$ ) at large distance. Utilizing a screening mechanism of a semi-permeable surface  $\eta$  we obtained a correct approximation of the forces at the different horizons (Table 3). However, the forces extend beyond the horizons resulting in a residual strong force necessary for the nuclear binding energy. To evaluate the forces between horizons, we consider in the next section the construction of a gravitational force potential providing a continuous solution for the screening mechanism.

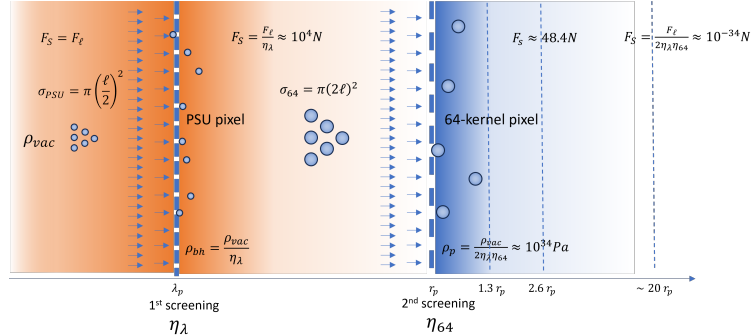


Figure 6: Semi-permeable surfaces at the two screening surfaces  $\lambda_p$  and  $r_p$  responsible for the vacuum fluctuations screening from  $\rho_{vac}$  to the proton black hole density  $\rho_{bh} = \frac{\rho_{vac}}{\eta_\lambda}$  and the rest mass energy density  $\rho_p = \frac{\rho_{vac}}{2\eta_\lambda\eta_{64}}$ . As described in section 4, the reduction in energy density is associated to a reduced 'gravity' pressure force  $F_p$  on the Planck plasma flow originating the color confinement force  $F_s \approx 10^4 N$  and the residual strong force  $F_s \approx 48.4 N$ .

## 4.5 Screening Potential $\varphi_g$

As seen in Table 3, the first screening of  $F_\ell$  reduces the pressure force of  $\rho_{vac}$  in the order of  $\alpha_g \sim 10^{-39}$  within the very short range, between the reduced Compton wavelength and the charge radius of the proton. To evaluate the forces close to the proton black hole exterior horizon  $\lambda_p$ , we consider the extended Schwarzschild solution by utilizing the regular solution given by the Kruskal-Szekeres (KS) coordinates which removes the artificial (mathematical) singularity at the black hole horizon  $r_s = \lambda_p$ . The resulting metric, giving the dynamics of the particle proper time near the horizon, shows a Yukawa-type interaction between a test particle and spacetime

$$ds^2 = \frac{4\lambda_p^3}{r} e^{-\frac{r}{\lambda_p}} (-dT^2 + dX^2) + r^2 d\Omega^2 \quad (4.25)$$

We will show that this Yukawa-type elasticity of spacetime (without the full treatment here) gives an accurate description of forces at the hadronic scale.

Furthermore, the Schwarzschild solution is typically applied to an 'empty' region (void of matter-energy) outside the horizon. However, the surrounding space of proton horizon  $\lambda_p$  is not empty as we have demonstrated that this region hosts the energy density equivalent to a black hole mass in terms of vacuum fluctuations. To model this presence of matter-energy in EFE, one can utilize either an equation of state, as we derived earlier, relating the pressure to the energy density, or a modified stress energy tensor derived from a Klein-Gordon (KG) field  $\varphi$  acting as a source term in EFE and resulting in [103]

$$T_{\mu\nu} = \frac{\rho_{vac}}{2} [\varphi^*_{;\mu}\varphi_{;\nu} + \varphi^*_{;\nu}\varphi_{;\mu} + g_{\mu\nu}(\varphi^*\varphi + \varphi^*_{;\alpha}\varphi^{;\alpha})] \quad (4.26)$$

The KG field models the relativistic waves interactions which are, in our case, Planck plasma turbulent vortical flow at the origin of mass. The KG field is associated to a divergence free 'particle-number' current  $J_\nu$  [104] describing the Planck plasma flow as

$$J_\nu = \frac{1}{2}i(\varphi^*_{;\nu}\varphi - \varphi_{;\nu}\varphi^*) \quad (4.27)$$

This full derivation of the Planck plasma flow circulation from EFE will be addressed in a later publication and for now, we consider a more direct approach by utilizing Yukawa-type energy potential reduction [53]. To be clear, so far we have obtained force values at specific discrete horizons, we now explore the mechanics of the continuous energy potential between horizons screening dynamics and their relationships. As a result to extend our analysis, we construct a general potential, as a first order approximation, as

$$\boxed{\varphi_g(r) = -\frac{Gm_\ell^2}{2r} \left( \alpha_g + \alpha_s e^{-\frac{r-r_p}{\lambda_p}} + \alpha_g^{-1} \frac{2\ell}{r} e^{-\frac{r-\lambda_p}{\ell}} \right)} \quad (4.28)$$

where  $\alpha_g$  is the gravitational coupling constant and  $\alpha_s$  the strong coupling constant. We utilize similar gravitational potentials as the ones published in [105] and [106] to illustrate and recover the forces reduction obtained by the energy-density screening. This general potential has been constructed as a superposition of three terms resulting from the two screening mechanisms

$$\varphi_g = \varphi_g^{(3)} + \varphi_g^{(2)} + \varphi_g^{(1)} \quad (4.29)$$

where  $\varphi_g^{(3)} = -\alpha_g \frac{Gm_\ell^2}{2r}$  corresponds to the Newtonian gravitational potential yielding the gravitational force between two proton rest masses. The second screening term  $\varphi_g^{(2)} = -\alpha_s \frac{Gm_\ell^2}{2r} e^{-\frac{r-r_p}{\lambda_p}}$  which leads to the color confinement force of the quark-antiquark interaction [99], is a Yukawa-type potential solution of a screened Poisson equation or time-independent Klein-Gordon equation of characteristic length  $\lambda_p$

$$\left( \Delta - \frac{1}{\lambda_p^2} \right) \varphi_g^{(2)}(r) = 0 \quad (4.30)$$

To evaluate the energy diffusion through the highly curved spacetime region of the proton interior, the system coupling Klein-Gordon equation with the Einstein field equations is generally utilized, which has been demonstrated to be equivalent in spherically symmetric gravitational field and in a semi-relativistic approximation to a Poisson-Schrödinger system [107].

The last term  $\varphi_g^{(1)} = -\alpha_g^{-1} \frac{Gm_\ell^2}{2r} \frac{2\ell}{r} e^{-\frac{r-\lambda_p}{\ell}}$ , corresponding to the first screening of the ground state Planck force is also a solution of a screened Poisson equation involving, in this case, a source term which would be expected as we have demonstrated it to be the source of mass

$$\left( \Delta - \frac{1}{\ell^2} \right) \varphi_g^{(1)}(r) = 2\alpha_g^{-1} \frac{Gm_\ell^2}{r^3} e^{-\frac{r-\lambda_p}{\ell}} \left[ 1 + \frac{\ell}{r} \right] \quad (4.31)$$

Given the Yukawa exponential attenuation on a characteristic length of the Planck length  $\ell$ , non-negligible solutions are localized at or near the Compton wavelength horizon, *i.e.* within a few Planck length after the horizon. Therefore, the source term can be computed at the lowest order where  $r \sim \lambda_p$  and  $\frac{\ell}{\lambda_p} \ll 1$  so that

$$2\alpha_g^{-1} \frac{Gm_\ell^2}{r^3} e^{-\frac{r-\lambda_p}{\ell}} \left[ 1 + \frac{\ell}{r} \right] \underset{r \sim \lambda_p}{\sim} 2\alpha_g^{-1} \frac{Gm_\ell^2}{\lambda_p^3} e^{-\frac{r-\lambda_p}{\ell}} \quad (4.32)$$

Utilizing the result of the holographic mass solution  $\alpha_g^{-1} = \frac{\lambda_p^2}{\ell^2}$  to elucidate the mechanism of the source term, we can write, ignoring the exponential for now,

$$2\alpha_g^{-1} \frac{Gm_\ell^2}{\lambda_p^3} = 16\pi \frac{M_p c^2}{A_\lambda} = \frac{16\pi}{3} \frac{\lambda_p}{c} \frac{\rho_{vac} c}{\eta_\lambda} = j_{bh} \tau_\lambda \quad (4.33)$$

where  $M_p$  is the proton black hole mass,  $A_\lambda = 4\pi\lambda_p^2$ ,  $\tau_\lambda = \frac{\lambda_p}{c}$  the characteristic time and  $j_{bh} = \frac{16\pi}{3} \frac{\rho_{vac} c}{\eta_\lambda}$  the mean energy flux per unit surface and unit time. From this derivation we can see that the source term is an energy flux per surface unit  $j_{bh}$  corresponding to the proton black hole energy radiated in the surrounding of the surface  $\lambda_p$  so that the screened Poisson equation for  $\varphi_g^{(1)}$  becomes

$$\left( \Delta - \frac{1}{\ell^2} \right) \varphi_g^{(1)}(r) = 16\pi \frac{M_p c^2}{A_\lambda} e^{-\frac{r-\lambda_p}{\ell}} \quad (4.34)$$

It is showing a direct relationship between quantum vacuum fluctuations and the surface energy diffused between the two horizons  $\lambda_p$  and  $r_p$ . That relationship is apparent in Figures 7 and 8 relating the Planck force to the confinement force and to the gravitational force.

## 4.6 Unification of forces from vacuum fluctuations as the source of color force and gravity

The force resulting from the potential  $\varphi_g$  is given by  $\vec{F}_s = -\vec{\nabla}\varphi_g$

$$F_s(r) = -\nabla_r \varphi_g = \frac{Gm_\ell^2}{2r^2} \left( \alpha_g + \alpha_s \left( 1 + \frac{r}{\lambda_p} \right) e^{-\frac{r-r_p}{\lambda_p}} + 2\alpha_g^{-1} \left( 1 + \frac{2\ell}{r} \right) e^{-\frac{r-\lambda_p}{\ell}} \right) \quad (4.35)$$

The derivation of  $F_s(r)$  allows us to recover the forces obtained for the different horizons at  $r = \lambda_p$  and  $r = r_p$  obtained in Table 3 such that

$$F_s(\lambda_p) \approx -\nabla_r \varphi_g^{(1)}(\lambda_p) = \alpha_g^{-1} \frac{Gm_\ell^2}{\lambda_p^2} = \frac{Gm_\ell^2}{\ell^2} = F_\ell \quad (4.36)$$

and the corresponding gravitational potential is

$$|\varphi_g(\lambda_p)| \approx |\varphi_g^{(1)}(\lambda_p)| = \frac{Gm_\ell^2}{\ell} = E_\ell \quad (4.37)$$

At the proton black hole horizon, the gravitational force and potential are ruled by the Planck force and Planck energy respectively as the source of mass and forces. At the Compton wavelength the energy potential  $\varphi_g^{(1)}$  dominates and  $\varphi_g^{(2)}$  and  $\varphi_g^{(3)}$  are negligible. However, as the radius increases towards the charge radius horizon, the force/energy density reduces so that  $\varphi_g^{(2)}$  eventually dominates at  $r_p$  such that

$$F_s(r_p) \approx -\nabla_r \varphi_g^{(2)}(r_p) = \frac{5}{2} \alpha_s \frac{Gm_\ell^2}{r_p^2} \quad (4.38)$$

To evaluate the strong coupling constant  $\alpha_s$ , we utilize the running coupling constant derivation of QCD asymptotic freedom [108]

$$\alpha_s(\mathcal{E}^2) \approx \frac{12\pi}{(33 - 2n_f) \ln \left( \frac{\mathcal{E}^2}{\Lambda^2} \right)} \approx 0.38 \quad (4.39)$$

where  $n_f = 6$  is the number of quarks active in pair production,  $\mathcal{E} = \frac{4\hbar c}{r_p} = 938$  MeV is the proton rest-mass energy and  $\Lambda^{(6)} \approx 89$  MeV is experimentally determined [97]. Therefore, we find

$$F_s(r_p) \approx \frac{Gm_\ell^2}{r_p^2} = \frac{F_\ell}{\eta_\lambda} \quad (4.40)$$

namely the color force as obtained in Table 3.

For radii  $r \gg r_p$  the general potential  $\varphi_g$  becomes dominated by  $\varphi_g^{(3)}$  the Newtonian gravitational potential where the force  $F_s(r)$  reduces to  $F_g(r)$  or the gravitational force between two protons at rest mass.

$$F_s(r) \xrightarrow{r \gg r_p} 2\alpha_g \frac{Gm_\ell^2}{(2r)^2} = 2 \frac{Gm_p^2}{(2r)^2} \quad (4.41)$$

$$|\varphi_g(r)| \xrightarrow{r \gg r_p} |\varphi_g^{(3)}(r)| = \frac{\alpha_g}{2} \frac{Gm_\ell^2}{r} = \frac{Gm_p^2}{2r} \quad (4.42)$$

The forces derived above have been established from the pressure force experienced by a PSU in the Planck plasma flow (Equation (4.9)) responsible for mass-energy. Thus, a physical interpretation of the energy potentials  $\varphi_g^{(1)}$ ,  $\varphi_g^{(2)}$  and  $\varphi_g^{(3)}$  is the surface energy per PSU, such that by summing the potential value of all the PSU of a screening surface one would recover a mass-energy on the order of the corresponding screening, namely the Planck mass for  $\varphi_g^{(1)} = m_\ell$ , the black hole mass for  $\varphi_g^{(2)} \eta_\lambda \sim M_p$  and the rest mass for  $\varphi_g^{(3)} \eta_{64} \sim m_p$ .

The force  $F_s$  is plotted on Figure 7, highlighting the dynamics of the two screenings from the ground state force  $F_\ell$  to the Newtonian gravitational force  $F_g$ . As the first screening has a characteristic length of the Planck length  $\ell$ , in a region of few Planck length after the horizon  $\lambda_p$  the force (and the potential) drops to the first screening value on the order of  $F_\ell/\eta_\lambda$  (and  $\frac{\alpha_s}{8} \frac{Gm_\ell^2}{r_p}$ ). Up to the charge radius the force and the potential are decreasing relatively slowly resulting in a force of  $\sim 10^4$  N at the proton charge radius (vertical red line in Figure 7). From there, the screening mechanism reduces the force dramatically again as we compute the approximate strength of this force relative to the electrostatic repulsion between two protons such as

$$F_s(r) = \frac{e^2}{4\pi\epsilon_0 r^2} \Leftrightarrow F_s(2.6 r_p) \approx 48.4 \text{ N} \quad (4.43)$$

The equilibrium is reached at a distance of  $r = 2.6 r_p \approx 2.18$  fm (vertical black line in Figure 7) yielding to the typical residual strong force estimate of  $F_s(2.6 r_p) \approx 48.4$  N. The distance we find for the equilibrium between the forces is in the range of the typical measured distance between two protons in  $\alpha$ -cluster given as  $\sim 1.9 - 2.4$  fm [109, 110]. Therefore, when we derive an analytical solution for the gravitational potential  $\varphi_g$  we find an effective distance of the force within a nucleus of a binding energy typically found for nucleon interaction on the order of the MeV.

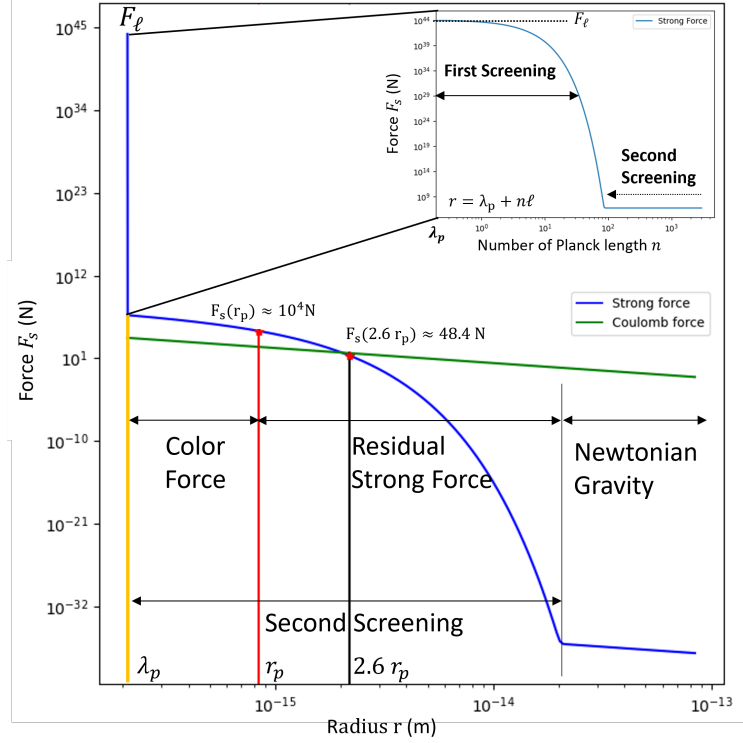


Figure 7: Color confinement force, residual strong force and gravitational force deriving from the general potential  $\varphi_g$ , illustrating the two screenings mechanism from the Planck force ground state  $F_\ell$ . The first screening profile is enlarged and plotted as a function of the number of Planck length from the Compton wavelength horizon  $\lambda_p$ . At  $r_p$ , we recover the measured color confinement force value of  $\approx 10^4$  N and at the typical inter-nucleon distance of  $2.6 r_p$  the 48.4 N range of the residual strong force.

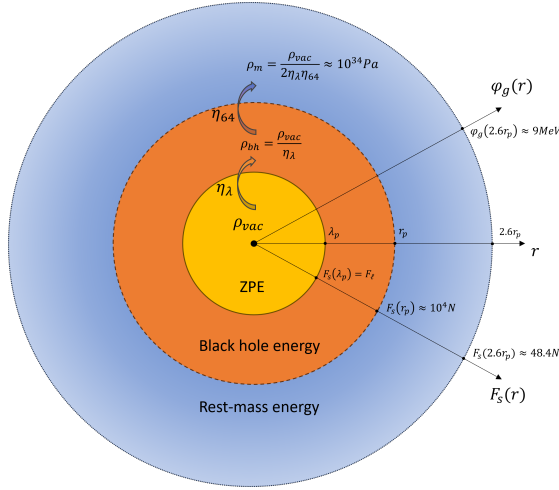


Figure 8: Summary of the Planck force screening at the horizons: reduced Compton wavelength of the proton  $\lambda_p$ , proton charge radius  $r_p$  and  $2.6 r_p$ , where the Planck force, the color confinement force and the residual strong force respectively occur.

## 5 Discussion

In this paper we have demonstrated that electromagnetic quantum vacuum fluctuations (or ZPE) are responsible for the energy curving spacetime resulting in the production of mass and forces. Historically, since the discovery of ZPE by Max Planck, it has been challenging to understand the impact of vacuum energy on the structure of spacetime, *i.e.* if quantum vacuum energy density is so high why is spacetime not curved into a very small regions with the rest of the universe. From our results, we demonstrate that indeed ZPE has curved spacetime into very small regions defined by Planck scale entities and that these entities collective behavior generate scaling so that at characteristic length the decoherence of the collective behavior results in residual energies (*i.e.* not all modes cancel out) that we measure and experience as masses and forces. Therefore, the application of such approach should be found to be scalable to vastly larger characteristic distances than the proton such as our universe as a whole. In fact, by applying the screening mechanism at the universe scale  $\eta_u$  and computing the universe density  $\rho_u$ <sup>12</sup> (Figure 10.a), we find the exact measured critical density at current time  $\rho_{crit} = \frac{3H_0^2}{8\pi G}$  which includes baryonic matter and so-called dark matter and dark energy [111]

$$\rho_u = \frac{\rho_{vac}}{\eta_u} = 8.53 \times 10^{-27} \text{ kg.m}^{-3} \quad (5.1)$$

where  $\eta_u = \frac{4\pi r_u^2}{\pi(\frac{c}{H_0})^2}$  the universe surface pixelization by PSU,  $r_u = \frac{c}{H_0}$  the radius of the observable universe and the Hubble constant typically given as  $H_0 = 67.4 \text{ km/s/Mpc}$  [112]. Therefore and remarkably, utilizing the same mechanism applied at the hadronic scale for the proton, when we screen  $\rho_{vac}$  with the Hubble horizon  $\eta_u$ , we obtain the exact critical density of the universe. Considering a single screening of  $\eta_u$  is equivalent to the Schwarzschild solution, it results that the observable universe of radius  $r_u$  obeys the Schwarzschild black hole condition as shown by [113] and [114]

$$\begin{aligned} M_u &= \frac{4}{3}\pi r_u^3 \times \rho_{crit} \\ &= \frac{r_u c^2}{2G} \end{aligned} \quad (5.2)$$

It is well-known since the early 2000 that supermassive black holes are present at the center of every large galaxy and that stellar black holes are common. Furthermore, primordial black holes theories are gaining significant popularity as a result of the latest measurements of James Webb Space Telescope [69]. Consequently, the life and evolution of galactic and stellar structures seem to have deep ties to black holes theory where, from the proton to the universe, black holes appears to be at the core of systems at all scales. Therefore, the Schwarzschild solution is the first natural scaling law for organized matter. In their review, Carr and Rees [60, 115] presented the black hole region as an upper limit towards which massive objects tend. The lower limit being the quantum realm with the wave-particle principle defining the proton Compton wavelength. Rees identifies a clear scaling from the instanton, which corresponds to the Planck scale region, to the universe demonstrating that the gravitational coupling constant  $\alpha_g^{-1} = \frac{\eta_u}{16}$  is the main scaling factor describing both mass and radius from the Planck scale to the size of the universe

$$m = \alpha_g^n m_p \quad (5.3)$$

where  $n$  is a rational number positive or negative. We note also that  $\alpha_g^{-1} m_p$  on Figure 9 represents the black hole energy at the Compton radius of the proton which Rees describes as the 'exploding hole' resulting from the Hawking evaporation scheme of primordial black holes which would exhaust their energy in the present epoch. However, from our result we have found a direct relationship of the energy phase transition from the

---

<sup>12</sup>Please note that in this section all densities are given in mass density due to the convention typically associated with cosmology.

density structure of the quantum vacuum to the black hole and rest-mass density resulting as demonstrated above to an evaporation time of  $10^{35}$  billion years. As well, Rees and Carr exploit the relationship between the proton and electron (the fine-structure constant  $\alpha$  and the mass ratio  $\mu = \frac{m_e}{m_p}$ ) to refine the scale. Such relationship was explored in the context of the holographic mass solution of the electron [116] where the mass of the electron is extracted from quantum vacuum fluctuations utilizing the same mechanism presented here.

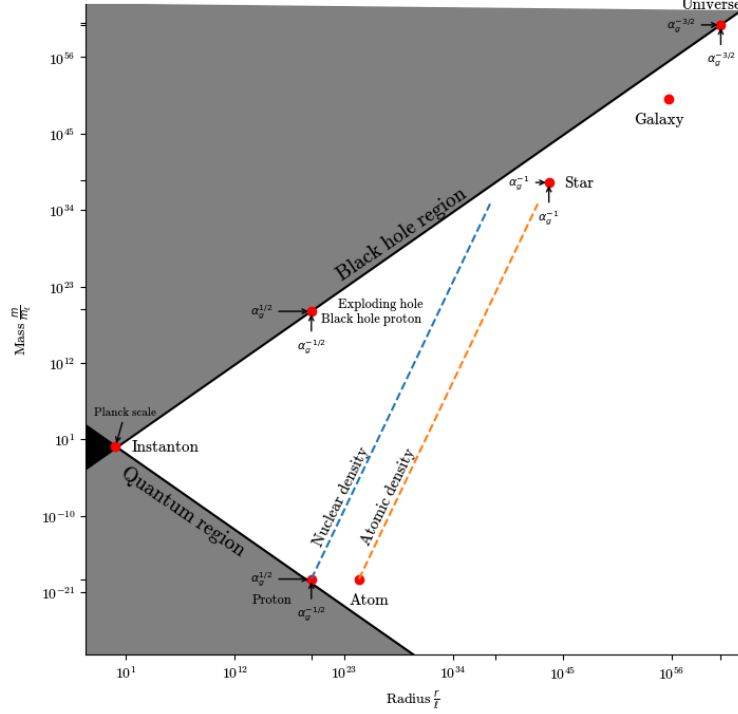


Figure 9: The figure is adapted from Carr and Rees scaling law [60]. It illustrates the atomic density line, the nuclear density line, the black hole density line and the 'quantum line' corresponding to the Compton wavelength. Most characteristic scales depend on simple powers of  $\alpha_g$  and the wide span of so many orders of magnitudes is a direct consequence of its huge numerical value which reflects the importance of gravity at all scales.

From a cosmogenesis perspective, the scaling law suggests that the scaling mechanism can be coupled with an evolutionary mechanism in which a universal horizon would emit a primordial Planck oscillator, as in Hawking radiation, which will find itself in an extremely low density external pressure environment resulting in a rapid inflation to a universal size causing internal vortical flows generating fractal structures at different scales [117, 118]. In such scenario, the growth would certainly go through a proton scale as composite matter creation and thermal cooling occur within the volume resembling the mechanism described in Einstein 'lost' paper of 1931 [119]. Consequently, a relationship between the vacuum internal energy structure of a proton size entity and the universe should be found (Figure 10.b). In fact, we find that the quantum vacuum fluctuations energy contained in the volume of a proton at the Compton wavelength  $\frac{h}{m_p c}$  is equivalent to the universe information-energy  $M_u$  (including the so-called dark energy and dark matter). For a Hubble constant  $H_0 = 67.4$  km/s/Mpc and where  $m_p^{vac}$  is the energy in the Compton wavelength volume of the proton, we get

$$\begin{aligned}
\frac{m_p^{vac}}{M_u} &= \frac{\rho_{vac} V_p}{\rho_{crit} V_u} \\
&= 16 \frac{H_0}{\ell^2 c} \left( \frac{h}{m_p c} \right)^3 \\
&\approx 1.03
\end{aligned} \tag{5.4}$$

Therefore, the quantum vacuum energy or information  $\rho_{vac}$  within a Compton proton volume is equivalent to the information or critical density  $\rho_{crit}$  in the universe. Furthermore, it should be noted that by utilizing the proton charge radius  $r_p$  instead of the Compton wavelength in the volume  $V_p$ , we find a value of 26.6% of the mass of the universe which is very close to the 26.8% typically given for the contribution of dark matter in the universe. This represents a direct conceptual holographic model of the information-energy both relating the quantum scale to the cosmological scale through vacuum fluctuations with very specific scaling factors and defining an entangle state of black holes hubs connected by a wormholes network as in  $ER = EPR$  [120, 121]. Furthermore, while the volume of a proton seems to hold an equivalence of information-energy in terms of vacuum fluctuations as the volume of our universe, the surface information of all protons  $N_p \eta_p$  is equivalent to the surface information of the universe  $\eta_u$  pixelized by kernel-64 such that  $\eta_u = \frac{4\pi r_u^2}{\pi(2\ell)^2} = \frac{r_u^2}{\ell^2}$  and utilizing Equation (5.4)

$$\frac{\eta_u}{N_p \eta_p} = \frac{m_p r_u^2}{M_u (\pi r_p)^2} \sim 1 \tag{5.5}$$

These last two computations imply not only an intimate relationship between protons and the universe but also demonstrate that the screening coefficient of a scale may have energy ratio relationships to much larger scales implying a fractal structure. In this case all the pixelization surfaces of the proton are equivalent to the screening of the quantum vacuum fluctuations resulting in the mass-energy density of the universe. Thus, the local holographic screening of a system has non-local relationships to other scales (fractal-like structure) in a network of information transfer that generates gradients across scales producing pressures or forces that we experience and measure both at the quantum scale and cosmological level. The scaling law emerging from the Planck plasma vortex flow and spacetime filaments results from the dynamic equilibrium of forces and energy density gradients between scales at different temperatures.

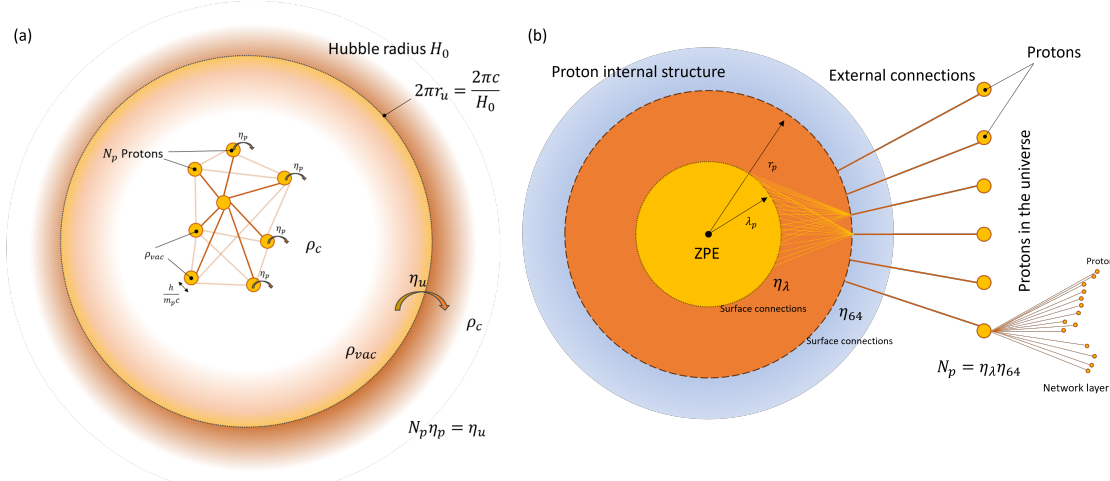


Figure 10: (a) Screening mechanism at the universe scale connecting the surface-information of the universe  $\eta_u$  to the surface-information of each proton  $\eta_p$ . (b) Relationship between the vacuum internal energy-information structure of a proton size entity to all the protons in the universe.

## Conclusion

We have demonstrated that the correlation functions for black-body radiation of the electromagnetic quantum vacuum fluctuations are the source of mass and forces at the hadronic scale. We have shown that a first screening mechanism of quantum vacuum fluctuations  $\rho_{vac}$  derived from the Planck scale discrete structure of an horizon recovers a direct analytical solution to Einstein's Field Equations in terms of the Schwarzschild solution at any scale, including the proton scale. This provides not only a deeper understanding of the quantum nature of spacetime producing gravitational curvature, but as well when applied to the proton scale, a source of energy at the origin of mass and forces. We have demonstrated as well that the Hawking radiation at the core at the reduced Compton wavelength of the proton corresponds to the rest mass energy of the proton and is equivalent to a second screening of  $\rho_{vac}$ . The gravitational curvature at the reduced Compton wavelength of the proton core results in the Planck force  $F_\ell$  at the horizon which undergoes a Yukawa-type potential generating the known measured values for the color confinement force, the residual strong force, the nuclear binding energy, and at about  $\sim 20$  fm the typical  $\sim 1/r^2$  Newtonian gravitational force.

The resulting unification of mass and forces derived from a Yukawa-type phase transitions of multiple screening horizons in the dynamics of the vacuum fluctuations lead to a clear picture of the gravitational quantization of space generating pressures and energy gradients at the origin of the structure of matter, the resulting quantum confinement and gravitational forces, and the agglomeration of organized matter, from the Planck scale to the universal scale. This can represent an important step toward achieving a long-sought goal in physics—an analytical and fundamental solution to quantum gravity.

## Acknowledgements

The authors would like to give a deep appreciation for the International Space Federation team for their invaluable support throughout the years and thoughtful discussions. Last but not least, we would like to thank the universe for its inspiring mathematical and physical beauty.

## References

1. Milonni, P. W. *An Introduction to Quantum Optics and Quantum Fluctuations* 1st ed. ISBN: 978-0-19-921561-4. doi:10.1093/oso/9780199215614.001.0001 (Oxford University Press Oxford, Jan. 31, 2019).
2. Wilczek, F. Scaling Mount Planck I: A View from the Bottom. *Physics Today* **54**, 12–13. ISSN: 0031-9228, 1945-0699. doi:10.1063/1.1387576 (June 2001).
3. Wilczek, F. Origins of mass. *Open Physics* **10**. ISSN: 2391-5471. doi:10.2478/s11534-012-0121-0 (Jan. 1, 2012).
4. Cho, A. Mass of the common quark finally nailed down. *Science Magazine* **201004**. doi:10.1126/article.30639 (2010).
5. Milonni, P. W. *The quantum vacuum: an introduction to quantum electrodynamics* (Academic press, 1993).
6. Lamoreaux, S. K. Demonstration of the Casimir force in the 0.6 to 6  $\mu$  m range. *Physical Review Letters* **78**, 5. doi:10.1103/PhysRevLett.78.5 (1997).
7. Bordag, M., Mohideen, U. & Mostepanenko, V. M. New Developments in the Casimir Effect. *Physics Reports* **353**, 1–205. ISSN: 03701573. doi:10.1016/S0370-1573(01)00015-1. arXiv: quant-ph/0106045 (Oct. 2001).
8. Wilson, C. M. *et al.* Observation of the dynamical Casimir effect in a superconducting circuit. *Nature* **479**, 376–379. ISSN: 1476-4687. doi:10.1038/nature10561 (Nov. 2011).
9. Lamb Jr, W. E. & Rutherford, R. C. Fine structure of the hydrogen atom by a microwave method. *Physical Review* **72**, 241. doi:10.1103/PhysRev.72.241 (1947).

10. STAR Collaboration *et al.* Measurement of  $e^+e^-$  Momentum and Angular Distributions from Linearly Polarized Photon Collisions. *Phys. Rev. Lett.* **127**. Publisher: American Physical Society, 052302. doi:10.1103/PhysRevLett.127.052302 (July 27, 2021).
11. Dirac, P. A. M. The quantum theory of the emission and absorption of radiation. *Proc. R. Soc. Lond. A* **114**, 243–265. ISSN: 0950-1207, 2053-9150. doi:10.1098/rspa.1927.0039 (Mar. 1927).
12. Anderson, C. D. The Apparent Existence of Easily Deflectable Positives. *Science* **76**, 238–239. ISSN: 0036-8075, 1095-9203. doi:10.1126/science.76.1967.238 (Sept. 9, 1932).
13. Schmitt, A. *et al.* Mesoscopic Klein-Schwinger effect in graphene. *Nat. Phys.* **19**, 830–835. ISSN: 1745-2473, 1745-2481. doi:10.1038/s41567-023-01978-9 (June 2023).
14. Planck, M. Über die Begründung des Gesetzes der schwarzen Strahlung. *Ann. Phys.* **342**, 642–656. ISSN: 00033804, 15213889. doi:10.1002/andp.19123420403 (1912).
15. Wesson, P. S. The application of dimensional analysis to cosmology: How to make cosmology simple by using dimensional conspiracy. *Space Science Reviews* **27**, 109–153 (1980).
16. Milonni, P. W. & Shih, M. .-. Zero-point energy in early quantum theory. *American Journal of Physics* **59**, 684–698. ISSN: 0002-9505, 1943-2909. doi:10.1119/1.16772 (Aug. 1991).
17. Mehra, J. *The Golden Age of Theoretical Physics: (Boxed Set of 2 Volumes)* ISBN: 978-981-02-4342-5. doi:10.1142/4454 (WORLD SCIENTIFIC, Feb. 2001).
18. Kragh, H. Walther Nernst: grandfather of dark energy? *Astronomy & Geophysics* **53**, 1.24–1.26. ISSN: 13668781. doi:10.1111/j.1468-4004.2012.53124.x (Feb. 2012).
19. Scully, M. O. & Zubairy, M. S. *Quantum optics* 630 pp. ISBN: 978-0-521-43458-4 (Cambridge University Press, Cambridge ; New York, 1997).
20. Kragh, H. *Dirac: a scientific biography* (Cambridge University Press, 1990).
21. Feynman, R. P. *QED: The strange theory of light and matter* (Princeton University Press, 1985).
22. Maldacena, J. & Susskind, L. Cool horizons for entangled black holes. *Fortschritte der Physik* **61**, 781–811. ISSN: 1521-3978. doi:10.1002/prop.201300020 (2013).
23. Hooft, G. in *Basics and Highlights in Fundamental Physics* 72–100 (World Scientific, 2001).
24. Bigatti, D. & Susskind, L. in *Strings, branes and gravity* 883–933 (World Scientific, 2001).
25. Wheeler, J. A. On the nature of quantum geometrodynamics. *Annals of Physics* **2**, 604–614. ISSN: 00034916. doi:10.1016/0003-4916(57)90050-7 (Dec. 1957).
26. Hawking, S. W. Virtual Black Holes. *Phys. Rev. D* **53**, 3099–3107. ISSN: 0556-2821, 1089-4918. doi:10.1103/PhysRevD.53.3099. arXiv: hep-th/9510029 (Mar. 15, 1996).
27. Sauter, F. Über das Verhalten eines Elektrons im homogenen elektrischen Feld nach der relativistischen Theorie Diracs. *Z. Physik* **69**, 742–764. ISSN: 1434-6001, 1434-601X. doi:10.1007/BF01339461 (Nov. 1931).
28. Schwinger, J. On Gauge Invariance and Vacuum Polarization. *Phys. Rev.* **82**, 664–679. ISSN: 0031-899X. doi:10.1103/PhysRev.82.664 (June 1, 1951).
29. Berdyugin, A. I. *et al.* Out-of-equilibrium criticalities in graphene superlattices. *Science* **375**. Publisher: American Association for the Advancement of Science, 430–433. doi:10.1126/science.abi8627 (Jan. 28, 2022).
30. Mignani, R. P. *et al.* Evidence of vacuum birefringence from the polarisation of the optical emission from an Isolated Neutron Star Feb. 14, 2018. arXiv: 1710.08709[astro-ph].
31. G, C. H. B. On the Attraction between Two Perfectly Conducting Plates. *Proc. Kon. Ned. Akad. Wet.* **51**, 793 (1948).
32. Dodonov, V. Fifty Years of the Dynamical Casimir Effect. *Physics* **2**, 67–104. ISSN: 2624-8174. doi:10.3390/physics2010007 (Feb. 14, 2020).

33. Moore, G. T. Quantum Theory of the Electromagnetic Field in a Variable-Length One-Dimensional Cavity. *Journal of Mathematical Physics* **11**, 2679–2691. ISSN: 0022-2488, 1089-7658. doi:10.1063/1.1665432 (Sept. 1, 1970).
34. Lähteenmäki, P., Paraoanu, G., Hassel, J. & Hakonen, P. J. Dynamical Casimir effect in a Josephson metamaterial. *Proceedings of the National Academy of Sciences* **110**, 4234–4238 (2013).
35. Vezzoli, S. *et al.* Optical analogue of the dynamical Casimir effect in a dispersion-oscillating fibre. *Communications Physics* **2**, 84 (2019).
36. Somers, D. A. T., Garrett, J. L., Palm, K. J. & Munday, J. N. Measurement of the Casimir torque. *Nature* **564**, 386–389. ISSN: 0028-0836, 1476-4687. doi:10.1038/s41586-018-0777-8 (Dec. 2018).
37. Kirchhoff, G. I. On the relation between the radiating and absorbing powers of different bodies for light and heat. *The London, Edinburgh, and Dublin Philosophical Magazine and Journal of Science* **20**, 1–21 (1860).
38. Einstein, A. Indeed, it seems to me that the observations regarding "blackbody radiation," photoluminescence, production of cathode rays by ultraviolet. *Annalen der Physik* **17**, 132–148 (1905).
39. Millikan, R. A. A direct photoelectric determination of Planck's "h". *Physical Review* **7**, 355 (1916).
40. Lehnert, B. Some Consequences of Zero Point Energy. *Journal of Electromagnetic Analysis and Applications* **06**. Number: 10 Publisher: Scientific Research Publishing, 319. doi:10.4236/jemaa.2014.610032 (2014).
41. Bethe, H. A. The Electromagnetic Shift of Energy Levels. *Phys. Rev.* **72**. Publisher: American Physical Society, 339–341. doi:10.1103/PhysRev.72.339 (Aug. 15, 1947).
42. Casimir, H. B. G. & Polder, D. The Influence of Retardation on the London-van der Waals Forces. *Phys. Rev.* **73**, 360–372. ISSN: 0031-899X. doi:10.1103/PhysRev.73.360 (Feb. 15, 1948).
43. Dirac, P. A. M. The quantum theory of the electron. *Proc. R. Soc. Lond. A* **117**, 610–624. ISSN: 0950-1207, 2053-9150. doi:10.1098/rspa.1928.0023 (Feb. 1928).
44. Breit, G. & Wheeler, J. A. Collision of two light quanta. *Physical Review* **46**, 1087 (1934).
45. Pike, O., Hill, E., Rose, S. & Mackenroth, F. *Observing the two-photon Breit-Wheeler process for the first time* 2014.
46. Anderson, P. W. Plasmons, gauge invariance, and mass. *Physical Review* **130**, 439 (1963).
47. Sakharov, A. D. *Vacuum quantum fluctuations in curved space and the theory of gravitation* Russian Academy of Sciences, 1967.
48. Thorne, K. S., Wheeler, J. A. & Misner, C. W. *Gravitation* (Freeman San Francisco, CA, 1971).
49. Shanahan, P. & Detmold, W. Pressure distribution and shear forces inside the proton. *Physical Review Letters* **122**, 072003. doi:10.1103/PhysRevLett.122.072003 (2019).
50. Burkert, V. D., Elouadrhiri, L. & Girod, F. X. The pressure distribution inside the proton. *Nature* **557**, 396–399. ISSN: 0028-0836, 1476-4687. doi:10.1038/s41586-018-0060-z (May 2018).
51. Haramein, N. *The Schwarzschild Proton Liege*, (Belgium), 2010.
52. Haramein, N. Quantum Gravity and the Holographic Mass (2013).
53. Yukawa, H. On the interaction of elementary particles. I. *Proceedings of the Physico-Mathematical Society of Japan. 3rd Series* **17**, 48–57. doi:10.11429/ppmsj1919.17.0\_48 (1935).
54. Dirac, P. A. M. Is there an Æther? *Nature* **168**, 906–907. ISSN: 0028-0836, 1476-4687. doi:10.1038/168906a0 (Nov. 1951).
55. Haramein, N. & Rauscher, E. A. THE ORIGIN OF SPIN: A CONSIDERATION OF TORQUE AND CORIOLIS FORCES IN EINSTEIN'S FIELD EQUATIONS AND GRAND UNIFICATION THEORY (2004).
56. Karsch, F. in *Lectures on quark matter* 209–249 (Springer, 2002). doi:10.1007/3-540-45792-5\_6.
57. Maiani, L. The J/Ψ as a probe of Quark-Gluon Plasma. *Lectures given at the International School of Subnuclear Physics, Trapani, Italy* (2004).

58. Rafelski, J. Discovery of quark-gluon plasma: strangeness diaries. *The European Physical Journal Special Topics* **229**, 1–140. doi:10.1140/epjst/e2019-900263-x (2020).
59. Rohlf, J. W. & Collings, P. J. Modern Physics from  $\alpha$  to Z 0. *Review Of" Modern Physics* **12**, 1–1994 (1994).
60. Carr, B. J. & Rees, M. J. The anthropic principle and the structure of the physical world. *Nature* **278**, 605–612. ISSN: 0028-0836, 1476-4687. doi:10.1038/278605a0 (Apr. 1979).
61. Bekenstein, J. D. Universal upper bound on the entropy-to-energy ratio for bounded systems. *Phys. Rev. D* **23**, 287–298. ISSN: 0556-2821. doi:10.1103/PhysRevD.23.287 (Jan. 15, 1981).
62. Wheeler, J. Information, physics, quantum: The search for link. Zurek (ed.) *Complexity, Entropy and the Physics of Information*, Addison-Wesley (1990).
63. Bekenstein, J. D. Black Holes and Entropy. *Phys. Rev. D* **7**, 2333–2346. ISSN: 0556-2821. doi:10.1103/PhysRevD.7.2333 (Apr. 15, 1973).
64. Haramein, N. Quantum Gravity and the Holographic Mass, Quantum. *Physical Review & Research International*, 2231–1815 (2013).
65. Gertsenshtein, M. Wave resonance of light and gravitational waves. *Sov Phys JETP* **14**, 84–85 (1962).
66. Landau, L. D., Lifshits, E. M. & Lifshits, E. M. *Mechanics* (CUP Archive, 1960).
67. Zel'dovich, Y. B. Electromagnetic and gravitational waves in a stationary magnetic field. *Zh. Eksp. Teor. Fiz.* **65**, 1311 (1973).
68. Schwarzschild, K. Über das Gravitationsfeld einer Kugel aus inkompressibler Flüssigkeit nach der Einsteinschen Theorie. *Sitzungsberichte der königlich preußischen Akademie der Wissenschaften zu Berlin*, 424–434 (1916).
69. Yuan, G.-W. *et al.* Rapidly growing primordial black holes as seeds of the massive high-redshift JWST Galaxies. *arXiv*. doi:10.48550/arXiv.2303.09391 (2023).
70. Harada, T., Yoo, C.-M. & Kohri, K. Threshold of primordial black hole formation. *Physical Review D* **88**, 084051. doi:10.1103/PhysRevD.88.084051 (2013).
71. Hawking, S. W. Gravitational Radiation from Colliding Black Holes. *Phys. Rev. Lett.* **26**, 1344–1346. ISSN: 0031-9007. doi:10.1103/PhysRevLett.26.1344 (May 24, 1971).
72. Einstein, A. & Rosen, N. The Particle Problem in the General Theory of Relativity. *Phys. Rev.* **48**, 73–77. ISSN: 0031-899X. doi:10.1103/PhysRev.48.73 (July 1, 1935).
73. Misner, C. W. & Wheeler, J. A. Classical physics as geometry. *Annals of Physics* **2**, 525–603. ISSN: 00034916. doi:10.1016/0003-4916(57)90049-0 (Dec. 1957).
74. Susskind, L. *Cosmic Natural Selection* July 29, 2004. arXiv: hep-th/0407266.
75. Wheeler, J. A. Geons. *Phys. Rev.* **97**, 511–536. ISSN: 0031-899X. doi:10.1103/PhysRev.97.511 (Jan. 15, 1955).
76. Wheeler, J. A. Assessment of Everett's "Relative State" Formulation of Quantum Theory. *Rev. Mod. Phys.* **29**, 463–465. ISSN: 0034-6861. doi:10.1103/RevModPhys.29.463 (July 1, 1957).
77. Wheeler, J. A. Geometrodynamics and the Problem of Motion. *Rev. Mod. Phys.* **33**, 63–78. ISSN: 0034-6861. doi:10.1103/RevModPhys.33.63 (Jan. 1, 1961).
78. Hawking, S. W. & Jackson, M. *A brief history of time* (Bantam books New York, 2001).
79. Hawking, S. W. Particle creation by black holes. *Communications in mathematical physics* **43**, 199–220 (1975).
80. Bardeen, J. M., Carter, B. & Hawking, S. W. The four laws of black hole mechanics. *Commun.Math. Phys.* **31**, 161–170. ISSN: 0010-3616, 1432-0916. doi:10.1007/BF01645742 (June 1973).
81. Hawking, S. W. Black hole explosions? *Nature* **248**, 30–31. ISSN: 0028-0836, 1476-4687. doi:10.1038/248030a0 (Mar. 1, 1974).
82. Antognini, A. *et al.* *Muonic-Atom Spectroscopy and Impact on Nuclear Structure and Precision QED Theory* Oct. 30, 2022. arXiv: 2210.16929[hep-ph, physics:nucl-th, physics:physics].

83. Xiong, W. *et al.* A small proton charge radius from an electron–proton scattering experiment. *Nature* **575**, 147–150 (2019).
84. Hammer, H.-W. & Meissner, U.-G. The proton radius: from a puzzle to precision. *arXiv preprint arXiv:1912.03881* (2019).
85. Xiong, W. & Peng, C. Proton Electric Charge Radius from Lepton Scattering. *Universe* **9**. Number: 4 Publisher: Multidisciplinary Digital Publishing Institute, 182. ISSN: 2218-1997. doi:10.3390/universe9040182 (Apr. 2023).
86. Karr, J.-P., Marchand, D. & Voutier, E. The proton size. *Nat Rev Phys* **2**, 601–614. ISSN: 2522-5820. doi:10.1038/s42254-020-0229-x (Sept. 30, 2020).
87. *Public Record Data 2012* <https://publicrecords.copyright.gov/detailed-record/25964136>.
88. Antognini, A. *et al.* Proton Structure from the Measurement of 2S-2P Transition Frequencies of Muonic Hydrogen. *Science* **339**, 417–420. ISSN: 0036-8075, 1095-9203. doi:10.1126/science.1230016 (Jan. 25, 2013).
89. Lin, Y.-H., Hammer, H.-W. & Meißner, U.-G. New Insights into the Nucleon’s Electromagnetic Structure. *Phys. Rev. Lett.* **128**. Publisher: American Physical Society, 052002. doi:10.1103/PhysRevLett.128.052002 (Feb. 3, 2022).
90. Gross, D. J. Nobel lecture: The discovery of asymptotic freedom and the emergence of QCD. *Reviews of Modern Physics* **77**, 837 (2005).
91. Wilczek, F. Getting its from bits. *Nature* **397**, 303–306. ISSN: 0028-0836, 1476-4687. doi:10.1038/16818 (Jan. 1999).
92. Dirac, P. A. M. Cosmological models and the large numbers hypothesis. *Mathematical and Physical Sciences* **338**, 439–446. doi:10.1098/rspa.1974.0095 (1974).
93. Dirac, P. in *Theories and Experiments in High-Energy Physics* 443–455 (Springer, 1975).
94. Wheeler, J. A. A journey into gravity and spacetime. *Scientific American Library* (1990).
95. Perko, H. *Introducing surface tension to spacetime* IOP Publishing, 2017.
96. Fritzsch, H. Quarks: the stuff of matter (1983).
97. Tanabashi, M. *et al.* Particle data group. *Phys. Rev. D* **98**, 030001. doi:pdg.lbl.gov/2018/reviews/rpp2018-rev-qcd.pdf (2018).
98. Baker, M. *et al.* The confining color field in SU (3) gauge theory. *The European Physical Journal C* **80**, 514. doi:10.1140/epjc/s10052-020-8077-5 (2020).
99. Griffiths, D. *Introduction to Elementary Particles* 286 (John Wiley & Sons, 1987).
100. Engelhardt, M., Langfeld, K., Reinhardt, H. & Tennert, O. Deconfinement in SU (2) Yang-Mills theory as a center vortex percolation transition. *Physical Review D* **61**, 054504 (2000).
101. Kamleh, W., Leinweber, D. B. & Virgili, A. Evidence that center vortices drive dynamical mass generation in QCD. *arXiv preprint arXiv:2305.18690* (2023).
102. Özel, F. & Freire, P. Masses, radii, and the equation of state of neutron stars. *Annual Review of Astronomy and Astrophysics* **54**, 401–440. doi:10.1146/annurev-astro-081915-023322 (2016).
103. Kaup, D. J. Klein-gordon geon. *Physical Review* **172**, 1331 (1968).
104. Kaup, D. J. Klein-Gordon Geon. *Phys. Rev.* **172**, 1331–1342. ISSN: 0031-899X. doi:10.1103/PhysRev.172.1331 (Aug. 25, 1968).
105. Kehagias, A. & Sfetsos, K. Deviations from the  $1/r^2$  Newton law due to extra dimensions. *Physics Letters B* **472**, 39–44. ISSN: 03702693. doi:10.1016/S0370-2693(99)01421-5. arXiv: hep-ph/9905417 (Jan. 2000).
106. Long, J. C., Chan, H. W. & Price, J. C. Experimental status of gravitational-strength forces in the sub-centimeter regime. *Nuclear Physics B* **539**, 23–34 (1999).

107. Giulini, D. & Großardt, A. The Schrödinger–Newton equation as a non-relativistic limit of self-gravitating Klein–Gordon and Dirac fields. *Class. Quantum Grav.* **29**, 215010. ISSN: 0264-9381, 1361-6382. doi:10.1088/0264-9381/29/21/215010 (Nov. 7, 2012).
108. Wilczek, F. Quantum Chromodynamics: The Modern Theory of the Strong Interaction. *Annu. Rev. Nucl. Part. Sci.* **32**, 177–209. ISSN: 0163-8998, 1545-4134. doi:10.1146/annurev.ns.32.120182.001141 (Dec. 1982).
109. Otsuka, T. *et al.*  $\alpha$ -Clustering in atomic nuclei from first principles with statistical learning and the Hoyle state character. *Nat Commun* **13**, 2234. ISSN: 2041-1723. doi:10.1038/s41467-022-29582-0 (Apr. 27, 2022).
110. Ebran, J.-P., Khan, E., Nikšić, T. & Vretenar, D. How atomic nuclei cluster. *Nature* **487**, 341–344. ISSN: 0028-0836, 1476-4687. doi:10.1038/nature11246 (July 19, 2012).
111. Haramein, N. & Baker, A. V. Resolving the vacuum catastrophe: a generalized holographic approach. *Journal of High Energy Physics, Gravitation and Cosmology* **5**, 412–424. doi:10.4236/jhepgc.2019.52023 (2019).
112. Sedgwick, T. M., Collins, C. A., Baldry, I. K. & James, P. A. The effects of peculiar velocities in SN Ia environments on the local H 0 measurement. *Monthly Notices of the Royal Astronomical Society* **500**, 3728–3742. doi:10.1093/mnras/staa3456 (2021).
113. Pathria, R. K. The Universe as a Black Hole. *Nature* **240**, 298–299. ISSN: 1476-4687. doi:10.1038/240298a0 (Dec. 1972).
114. Popławski, N. in *Regular Black Holes: Towards a New Paradigm of Gravitational Collapse* 485–499 (Springer, 2023). doi:10.1007/978-981-99-1596-5\_13.
115. Dicke, R. H. Dirac’s Cosmology and Mach’s Principle. *Nature* **192**. Number: 4801 Publisher: Nature Publishing Group, 440–441. ISSN: 1476-4687. doi:10.1038/192440a0 (Nov. 1961).
116. Baker, A., Haramein, N. & Alirol, O. The electron and the holographic mass solution. *Physics Essays* **32** (2019).
117. Zhu, W. & Feng, L.-l. Vortical Motions of Baryonic Gas in the Cosmic Web: Growth History and Scaling Relation. *The Astrophysical Journal* **811**, 94 (2015).
118. Parker, M. C. & Jeynes, C. Maximum Entropy (Most Likely) Double Helical and Double Logarithmic Spiral Trajectories in Space-Time. *Sci Rep* **9**, 10779. ISSN: 2045-2322. doi:10.1038/s41598-019-46765-w (July 25, 2019).
119. Castelvecchi, D. *et al.* Einstein’s lost theory uncovered. *Nature* **506**, 418–419 (2014).
120. Kain, B. Probing the connection between entangled particles and wormholes in general relativity. *Physical Review Letters* **131**, 101001. doi:10.1103/PhysRevLett.131.101001 (2023).
121. Haramein, N., Brown, W. D. & Val Baker, A. The Unified Spacememory Network: from Cosmogenesis to Consciousness. *Neuroquantology* **14**. ISSN: 13035150 (June 29, 2016).
122. Adler, R. J., Casey, B. & Jacob, O. C. Vacuum catastrophe: An elementary exposition of the cosmological constant problem. *American Journal of Physics* **63**, 620–626. ISSN: 0002-9505, 1943-2909. doi:10.1119/1.17850 (July 1995).

## Appendix A: Energy of the free electromagnetic field<sup>13</sup>

In free space, the electromagnetic oscillating field describes by the gauge invariant transverse vector potential  $\vec{A}(\vec{r}, t)$  satisfies the homogeneous wave equation and the divergence condition (utilizing the Coulomb Gauge assumption)

$$\vec{\nabla}^2 \vec{A} - \frac{1}{c^2} \frac{\partial^2}{\partial t^2} \vec{A} = 0$$

$$\vec{\nabla} \cdot \vec{A} = 0$$

The simplest nontrivial solution for those two equations is given by

$$\vec{A}(\vec{r}, t) = \sum_{\vec{k}, s} \sqrt{\frac{\hbar}{2\epsilon_0\omega_{\vec{k}}\mathcal{V}}} \left( a_{\vec{k}}(t) A_{\vec{k}}(\vec{r}) + a_{\vec{k}}^\dagger(t) A_{\vec{k}}^*(\vec{r}) \right)$$

with

$$a_{\vec{k}}(t) = -i\omega_{\vec{k}} a_{\vec{k}}(t)$$

and each  $A_{\vec{k}}$  is a solution of the Helmholtz equation

$$\vec{\nabla}^2 \vec{A}_{\vec{k}} + \frac{\omega_{\vec{k}}^2}{c^2} \frac{\partial^2 \vec{A}_{\vec{k}}}{\partial t^2} = \vec{0}$$

The operators  $a_{\vec{k}}$  and  $a_{\vec{k}}^\dagger$  are usually named annihilation and creation operators. And the electric  $\vec{E}$  and magnetic  $\vec{B}$  fields are given by

$$\vec{E} = -\frac{\partial \vec{A}}{\partial t}$$

$$\vec{B} = \vec{\nabla} \times \vec{A}$$

The Hamiltonian of such electromagnetic oscillating field is

$$\hat{H} = \frac{1}{2} \int_{\mathcal{V}} \epsilon_0 (E^2 + c^2 B^2) d^3 r = 2\epsilon_0 \sum_{\vec{k}, s} \omega_{\vec{k}, s}^2 |\alpha_{\vec{k}, s}(t)|^2$$

where  $s$  define the polarization mode and the time dependent wave amplitude  $\alpha_{\vec{k}, s}(t)$  is given by

$$\alpha_{\vec{k}, s}(t) = \sqrt{\frac{\hbar}{2\epsilon_0\omega_{\vec{k}}}} a_{\vec{k}}(t)$$

The energy of a system of independent harmonic oscillators, one representing each mode  $(\vec{k}, s)$  of the electromagnetic free field. The state of the classical radiation field is specified by the set of all canonical variables position-momentum  $(q_{\vec{k}, s}, p_{\vec{k}, s})$  is given by

---

<sup>13</sup>Appendix A and B were both adapted from [1]

$$\hat{H} = \frac{1}{2} \sum_{\vec{k}} \sum_s \left[ p_{\vec{k},s}^2(t) + \omega^2 q_{\vec{k},s}^2(t) \right]$$

where

$$q_{\vec{k},s} = i\sqrt{\epsilon_0}(\alpha_{\vec{k},s} - \alpha_{\vec{k},s}^*)$$

$$p_{\vec{k},s} = \omega_{\vec{k},s}\sqrt{\epsilon_0}(\alpha_{\vec{k},s} + \alpha_{\vec{k},s}^*)$$

Then, the quantized hamiltonian takes the following form

$$H = \frac{1}{2} \sum_{\vec{k},s} \hbar\omega_k \left( a_{\vec{k},s}^\dagger a_{\vec{k},s} + a_{\vec{k},s} a_{\vec{k},s}^\dagger \right) = \sum_{\vec{k},s} \hbar\omega_k \left( a_{\vec{k},s}^\dagger a_{\vec{k},s} + \frac{1}{2} \right) = \sum_{\vec{k},s} \hbar\omega_k \left( n_{\vec{k},s} + \frac{1}{2} \right)$$

where the photon number operator  $n_{\vec{k},s} = a_{\vec{k},s}^\dagger a_{\vec{k},s}$  gives the number of photon at the energy level  $E_n$ . The electric field operator is

$$E(t) = -\frac{\partial \vec{A}}{\partial t} = i \sum_{\vec{k},s} \sqrt{\frac{\hbar\omega}{2\epsilon_0\mathcal{V}}} \left( a_{\vec{k}}(t) A_{\vec{k}}(\vec{r}) - a_{\vec{k}}^\dagger(t) A_{\vec{k}}^*(\vec{r}) \right)$$

In the vacuum state  $|0\rangle$  (state with 0 photon), the mean values of the electric and magnetic fields are given by

$$\langle 0 | \vec{E}_H(\vec{r},t) | 0 \rangle = i \sqrt{\frac{\hbar}{2\epsilon_0\mathcal{V}}} \sum_k \sum_{s=1}^2 \sqrt{\omega_k} \left[ \langle 0 | a_{\vec{k},s} \vec{e}_s(\vec{k}) e^{i(\vec{k} \cdot \vec{r} - \omega_k t)} | 0 \rangle + \langle 0 | a_{\vec{k},s}^\dagger \vec{e}_s^*(\vec{k}) e^{-i(\vec{k} \cdot \vec{r} - \omega_k t)} | 0 \rangle \right]$$

$$= 0$$

because

$$\langle 0 | a_{\vec{k},s} | 0 \rangle = 0$$

$$\langle 0 | a_{\vec{k},s}^\dagger | 0 \rangle = 0$$

Thus,

$$\boxed{\langle 0 | \vec{E}_H(\vec{r},t) | 0 \rangle = \langle 0 | \vec{B}_H(\vec{r},t) | 0 \rangle = 0}$$

The electromagnetic field mean value is zero but its fluctuations is not zero as shown for one mode by

$$E(t) = \sqrt{\frac{\hbar\omega}{2\epsilon_0\mathcal{V}}} (ae^{-i\omega t} + a^\dagger e^{i\omega t})$$

$$E^2(t) = \frac{\hbar\omega}{2\epsilon_0\mathcal{V}} (a^2 e^{-i2\omega t} + (a^\dagger)^2 e^{i2\omega t} + 2a^\dagger a + I)$$

Taking the mean value, we get

$$\langle 0 | a^2 | 0 \rangle = \langle 0 | (a^\dagger)^2 | 0 \rangle = \langle 0 | aa^\dagger | 0 \rangle = 0$$

Thus, we find the vacuum energy in the free space for the pulsation  $\omega$

$$\boxed{\langle 0 | E^2(t) | 0 \rangle = \frac{1}{2} \frac{\hbar\omega}{\epsilon_0 \mathcal{V}}}$$

To compute the effective energy density, we need to consider the correlation function.

## Appendix B : Correlation function and black body radiation

We can use the density operator to evaluate the second order correlation functions of the optical field

$$\begin{aligned} \left\langle \vec{E}^{(-)}(\vec{r}, t) \cdot \vec{E}^{(+)}(\vec{r}, t + \tau) \right\rangle &= \sum_k \sum_{s=1}^2 \frac{\hbar\omega_{\vec{k}}}{2\epsilon_0 \mathcal{V}} \frac{e^{-i\omega_{\vec{k}}\tau}}{e^{\hbar\omega_{\vec{k}}/k_B T} - 1} \\ \left\langle \vec{E}^{(+)}(\vec{r}, t) \cdot \vec{E}^{(-)}(\vec{r}, t + \tau) \right\rangle &= \sum_k \sum_{s=1}^2 \frac{\hbar\omega_{\vec{k}}}{2\epsilon_0 \mathcal{V}} \frac{e^{-i\omega_{\vec{k}}\tau}}{e^{\hbar\omega_{\vec{k}}/k_B T} - 1} \end{aligned}$$

where the single polarization component of the electric field operator ( $s = "+"$  and  $s = "-"$ ) are

$$\begin{aligned} \vec{E}^{(+)}(\vec{r}, t) &= i \sum_{\vec{k}} \sqrt{\frac{\hbar\omega}{2\epsilon_0 \mathcal{V}}} a_{\vec{k}} e^{-i\omega_{\vec{k}}t} = \vec{E}^{(-)}(\vec{r}, t)^\dagger \\ \vec{E}^{(-)}(\vec{r}, t) &= -i \sum_{\vec{k}} \sqrt{\frac{\hbar\omega}{2\epsilon_0 \mathcal{V}}} a_{\vec{k}}^* e^{i\omega_{\vec{k}}t} \end{aligned}$$

It results the normally ordered field correlation functions is

$$\left\langle \vec{E}^{(-)}(\vec{r}, t) \cdot \vec{E}^{(+)}(\vec{r}, t + \tau) \right\rangle = \sum_{\vec{k}} \frac{\hbar\omega}{2\epsilon_0 \mathcal{V}} \langle n_{\vec{k}} \rangle e^{-i\omega\tau} = \sum_{\vec{k}} \frac{\hbar\omega}{2\epsilon_0 \mathcal{V}} \langle a_{\vec{k}}^\dagger a_{\vec{k}} \rangle e^{-i\omega\tau}$$

and the anti-normally ordered correlation function is

$$\left\langle \vec{E}^{(+)}(\vec{r}, t) \cdot \vec{E}^{(-)}(\vec{r}, t + \tau) \right\rangle = \sum_{\vec{k}} \frac{\hbar\omega}{2\epsilon_0 \mathcal{V}} \langle a_{\vec{k}} a_{\vec{k}}^\dagger \rangle e^{i\omega\tau} = \sum_{\vec{k}} \frac{\hbar\omega}{2\epsilon_0 \mathcal{V}} (\langle n_{\vec{k}} \rangle + 1) e^{i\omega\tau}$$

The creation annihilation operator for the mode  $\vec{k}$  gives

$$\langle a_{\vec{k}} a_{\vec{k}}^\dagger \rangle = \langle a_{\vec{k}}^\dagger a_{\vec{k}} \rangle + 1 = \langle n_{\vec{k}} \rangle + 1 = \frac{1}{e^{\hbar\omega_{\vec{k}}/k_B T} - 1} + 1 = \frac{e^{\hbar\omega_{\vec{k}}/k_B T}}{e^{\hbar\omega_{\vec{k}}/k_B T} - 1}$$

where  $n_{\vec{k}}$  is the photon number operator for the mode  $\vec{k}$  and  $\langle n_{\vec{k}} \rangle = \langle a_{\vec{k}}^\dagger a_{\vec{k}} \rangle$  is the average photon number of mode  $\vec{k}$ .

A coherent system yields symmetrically ordered correlation function corresponding to the sum of the normally and anti-normally ordered correlation functions which results in the continuous mode in

$$\begin{aligned}\langle \vec{E}(\vec{r}, t) \cdot \vec{E}(\vec{r}, t + \tau) \rangle &= \langle \vec{E}^{(-)}(\vec{r}, t) \cdot \vec{E}^{(+)}(\vec{r}, t + \tau) \rangle + \langle \vec{E}^{(+)}(\vec{r}, t) \cdot \vec{E}^{(-)}(\vec{r}, t + \tau) \rangle \\ &= \frac{\hbar}{\pi\epsilon_0 c^3} \int_0^\infty \left( \frac{e^{-i\omega\tau}}{e^{\hbar\omega/k_B T} - 1} + \frac{e^{i\omega\tau}}{e^{\hbar\omega/k_B T} - 1} + e^{i\omega\tau} \right) \omega^3 d\omega \\ &= \frac{2\hbar}{\pi\epsilon_0 c^3} \int_0^\infty \frac{\cos \omega\tau}{e^{\hbar\omega/k_B T} - 1} \omega^3 d\omega + \frac{\hbar}{\pi\epsilon_0 c^3} \int_0^\infty e^{i\omega\tau} \omega^3 d\omega\end{aligned}$$

The temperature-dependent term can be calculated as

$$\frac{2\hbar}{\pi\epsilon_0 c^3} \int_0^\infty \frac{\cos \omega\tau}{e^{\hbar\omega/k_B T} - 1} \omega^3 d\omega = \frac{2\hbar}{\pi\epsilon_0 c^3} \left( \frac{b^4}{\sinh^2(b\tau)} \left[ \frac{3}{\sinh^2(b\tau)} + 2 \right] - \frac{3}{\tau^4} \right)$$

where  $b = \frac{\pi k_B T}{\hbar}$ . The temperature-independent term can be evaluated as [1]

$$\frac{\hbar}{\pi\epsilon_0 c^3} \int_0^\infty e^{i\omega\tau} \omega^3 d\omega = \frac{2\hbar}{\pi\epsilon_0 c^3} \times \frac{3}{\tau^4}$$

such that the total energy of the symmetrically ordered system is

$$\epsilon_0 \langle \vec{E}(\vec{r}, t) \cdot \vec{E}(\vec{r}, t + \tau) \rangle = \frac{2\hbar}{\pi c^3} \frac{b^4}{\sinh^2(b\tau)} \left[ \frac{3}{\sinh^2(b\tau)} + 2 \right]$$

and in the limit case of  $T \rightarrow 0$  K

$$\epsilon_0 \langle \vec{E}(\vec{r}, t) \cdot \vec{E}(\vec{r}, t + \tau) \rangle \xrightarrow{T \rightarrow 0} \frac{6\hbar}{\pi c^3} \times \frac{1}{\tau^4} = \rho_{vac} \left( \frac{t_\ell}{\tau} \right)^4$$

## Appendix C: Non commutativity of canonical operators

From the definition of the position and momentum operators we have :

$$\begin{aligned}\hat{x} &= i\sqrt{\frac{\hbar}{2m\omega}}(a - a^\dagger) \\ \hat{p} &= \sqrt{\frac{m\omega\hbar}{2}}(a + a^\dagger)\end{aligned}$$

Thus for a vector  $|n\rangle$  the commutator applies as

$$\begin{aligned}\langle n | [\hat{x}, \hat{p}] | n \rangle &= \frac{i\hbar}{2} \langle n | [a - a^\dagger, a + a^\dagger] | n \rangle \\ &= \frac{i\hbar}{2} \langle n | (a - a^\dagger)(a + a^\dagger) - (a + a^\dagger)(a - a^\dagger) | n \rangle \\ &= \frac{i\hbar}{2} \langle n | a^2 + aa^\dagger - a^\dagger a - a^{\dagger 2} - a^2 + aa^\dagger - a^\dagger a + a^{\dagger 2} | n \rangle \\ &= i\hbar \langle n | aa^\dagger - a^\dagger a | n \rangle \\ &= i\hbar\end{aligned}$$

From [5] (p53) we have the position

$$x(t) = -\frac{e}{m} \frac{E_0 \omega e^{-i\omega t + \theta}}{(\omega^2 - \omega_0^2) + i\tau\omega^3}$$

where  $\tau = 2e^2/3mc^3\epsilon_0$  and

$$\dot{x}(t) = -i\omega x(t)$$

We note that  $\hat{x}|x\rangle = x|x\rangle$ ,  $\langle x|\hat{x} = (\hat{x}^\dagger|x\rangle)^\dagger = x^*\langle x|$  and  $\hat{p}|x\rangle = m\dot{x}|x\rangle$ . Thus

$$\begin{aligned} \langle [\hat{x}, \hat{p}] \rangle_\omega &= \langle x | [\hat{x}, \hat{p}] | x \rangle \\ &= \langle x | \hat{x}\hat{p} - \hat{p}\hat{x} | x \rangle \\ &= \langle x | \hat{x}\hat{p} | x \rangle - \langle x | \hat{p}\hat{x} | x \rangle \\ &= mx^*\dot{x} - m\dot{x}^*x \\ &= -2mi\omega|x|^2 \\ &= -2\frac{ie^2 E_0^2}{m} \frac{\omega}{(\omega^2 - \omega_0^2)^2 + \tau^2\omega^6} \end{aligned}$$

Using  $\sum_\omega \rightarrow \frac{1}{4\pi^2} \int \omega^2 d\omega$  and  $E_{0\omega}^2 = \frac{8\pi}{3\epsilon_0} B_0(\omega) d\omega = \frac{8\pi\hbar}{3\epsilon_0\pi c^3} \omega^3 d\omega$  it follows by noticing that the equation is peaked in  $\omega \sim \omega_0$

$$\begin{aligned} [\hat{x}, \hat{p}] &= \frac{ie^2\hbar}{2\pi^2\epsilon_0 mc^3} \frac{8\pi}{3} \int_0^\infty \frac{d\omega \omega^4}{(\omega^2 - \omega_0^2)^2 + \tau^2\omega^6} \\ &\simeq \frac{2i\hbar e^2}{3\pi\epsilon_0 mc^3} \omega_0^3 \int_{-\infty}^\infty \frac{dx}{x^2 + \tau^2\omega^6} \\ &= \frac{2i\hbar e^2 \omega_0^3}{3\pi\epsilon_0 mc^3} \frac{\pi}{\tau\omega_0^3} \\ &= i\hbar \end{aligned}$$

where  $x = \omega^2 - \omega_0^2$

## Appendix D: ZPE Calculation

The ZPE density derives from the sum of elementary spherical harmonic oscillators with ground state energy  $E_0$  on all possible modes of the fields (See Appendix B). For three dimensional spherical oscillators

$$E_0(\omega) = \frac{3}{2}\hbar\omega$$

and the vacuum energy density results from the sum of all the mode of energy  $E_0(\omega)$ :

$$\rho_{vac} = \frac{1}{V} \sum_\omega n(\omega) E_0(\omega)$$

with  $n(\omega)$  the number of mode of pulsation  $\omega$ . Following the calculation derived by Adler *et al* in [122], we calculate the number of modes  $dn$  between  $\omega$  and  $\omega + d\omega$  in a volume  $V$  as the volume of momentum of space in a thin spherical shell, divided by  $(2\pi)^3$ , such that

$$dn(\omega) = \frac{V}{c^3(2\pi)^3} 4\pi\omega^2 d\omega$$

and therefore, by switching the sum into integral we have

$$\rho_{vac} = \frac{2\pi}{V} \int_0^{\omega_{max}} E_0(\omega) dn(\omega) = \frac{3}{2}\hbar \int_0^{\omega_{max}} \frac{8\pi^2\omega^3}{c^3(2\pi)^3} d\omega = \frac{3}{8\pi} \frac{\hbar\omega_{max}^4}{c^3}$$

The adjunction of  $2\pi$  is added as a geometrical factor. One would expect an infinity of possible mode ( $\omega_{max} \rightarrow \infty$ ) such that the vacuum density  $\rho_{vac}$  would diverge. However, as explained in Appendix C, we limit the large frequencies to a oscillation cut-off pulsation corresponding to an oscillator of characteristic diameter  $\ell$ , the planck length, we obtain a cut-off pulsation  $\omega_{max} = \frac{2\pi c}{2\pi \frac{\ell}{2}} = \frac{2c}{\ell}$ . And thus, the vacuum energy density is finite and can be expressed as (in unity of mass) :

$$\rho_{vac} = \frac{6}{\pi} \frac{c^5}{G^2 \hbar} = 9.89 \times 10^{96} \text{ kg/m}^3$$

(5.6)

The choice of the cut-off  $\omega_{max} = \frac{2c}{\ell}$  is justified by considering the Planck length scale as the minimum acceptable length in our space time structure as described in section 2.2.

## Appendix E: metric gradient $\frac{\partial g_{rr}}{\partial r}$

For the Schwarzschild metric we have

$$g_{rr} = \frac{1}{1 - \frac{r_s}{r}}$$

and the derivative of  $g_{rr}$  along the  $r$  coordinate is

$$\frac{\partial g_{rr}}{\partial r} = \frac{r_s}{r^2} \frac{1}{\left(1 - \frac{r_s}{r}\right)^2} = \frac{r_s}{(r - r_s)^2} \sim \frac{r_s}{r^2}$$

Therefore, a small perturbation of the metric in the radial direction outside the Schwarzschild radius less than the unity

$$\delta g = \frac{r_s \delta r}{r^2} \leq 1$$